https://doi.org/10.5194/amt-2024-57
Preprint. Discussion started: 13 May 2024

Atmospheric Measurement Techniques Discussions

CIAO observatory main upgrade: building up an ACTRIS compliant aerosol in-situ laboratory

Teresa Laurita[1], Alessandro Mauceri[1], Francesco Cardellicchio[1], Emilio Lapenna[1], Benedetto De Rosa[1], Serena Trippetta[1], Michail Mytilinaios[1], Davide Amodio[1], Aldo Giunta[1], Ermann Ripepi[1], Canio Colangelo[1], Nikolaos Papagiannopoulos[1], Francesca Morrongiello[1], Claudio Dema[1], Simone Gagliardi[1], Carmela Cornacchia[1], Rosa Maria Petracca Altieri[1], Aldo Amodeo[1], Marco Rosoldi[1], Donato Summa[1], Gelsomina Pappalardo[1], Lucia Mona[1]

[1]Consiglio Nazionale delle Ricerche – Istituto di Metodologie per l'Analisi Ambientale CNR-IMAA, C. da S. Loja, Tito Scalo, Potenza, 85050, Italy

Correspondence to: Teresa Laurita (teresa.laurita@cnr.it)

Abstract

This paper describes the aerosol in-situ laboratory at CIAO (CNR IMAA Atmospheric Observatory) in South Italy, outlining its configuration and detailing each instrument and sampling lines. The CIAO observatory has been collecting observations of atmospheric components since 2000. Initially the activities revolved around aerosol lidar, later radiosounding and cloud remote sensing observations were added over the years and made CIAO a leading atmospheric observatory in the Mediterranean region. In 2018, a significant upgrade started for enhancing the observational capability by adding aerosol in-situ instruments, with the objective to push new research boundaries for aerosol characterization and multi-instrumental synergistic approaches. Here, we describe each technical implementation step for building up an extensive aerosol in-situ laboratory compliant with ACTRIS (Aerosol Clouds and Trace gases Research InfraStructure) standard operating procedures. Starting from scratch, the long path initiated in 2018, with the design of the laboratory in terms of instruments, container organization, inlets and sampling lines optimizations, that required time and interactions with experts in the field. Reporting here all the details about the final solutions implemented at CIAO, this paper will be, for new aerosol in-situ laboratory, a practical guide for the implementation of the aerosol in-situ observational site.

1 Introduction

The importance of a quantitative and qualitative assessment of atmospheric aerosol characteristics has been recognized since many years: aerosols are responsible for direct and indirect effects on atmospheric processes, affecting climate and human health, as well as precipitation cycle and air quality (e.g. Pöschl, 2005). Depending on their sources, aerosols appear in different sizes/shapes and their relatively short lifetime makes the physical and chemical properties extremely variable both on temporal

https://doi.org/10.5194/amt-2024-57
Preprint. Discussion started: 13 May 2024


Atmospheric Measurement Techniques Discussions

and spatial scales. Because of the inherent complexity of aerosols, a single measurement technique providing all the relevant information is not available: thus, a multi-instrument approach is needed. The combination of different techniques and observational platforms can be crucial for a better understanding of the presence and the characteristics of atmospheric aerosols, as well as their role in the large variety of processes in which they are involved. Aerosol Clouds and Trace Gases Research InfraStructure (ACTRIS, www.actris.eu) is the European Research Infrastructure (RI) aiming to integrate previous existing networks for the characterization of aerosols, clouds and trace gases using and integrating in-situ and remote sensing observations, and experimental platforms for the characterization of atmospheric components under controlled environments. An overarching investigation of the atmosphere which accounts for all these three components is a winning strategy: For instance, aerosols act as cloud condensation nuclei (CNN) affecting the cloud properties and lifetime; emitted gas species may act as precursors to form new particles in the atmosphere, i.e., the secondary aerosol. Integrated approaches of remote sensing and in-situ observations allows to take the most from the detailed and accurate characterization in terms of morphology of particles, dimension and chemical composition: the remote sensing provide the vertical profile of physical and optical properties information which are essential for investigating aerosol layers, long range transportation, mixing processes and aerosol-cloud interactions; the latter is the only approach to provide the chemical composition and reliable data at ground level, where aerosols affect ecosystems and humans.

In this scenario, the CNR-IMAA (Consiglio Nazionale delle Ricerche – Istituto di Metodologie per l'Analisi Ambientale) Atmospheric Observatory (CIAO; Madonna et al., 2011), operating since 2000, has been recently upgraded with the aerosol in-situ observational component, thus complementing the multi-year high-quality aerosol remote sensing data record. The combination of the aerosol in-situ measurements with remote sensing observations is expected to strengthen fundamental knowledge about aerosol impact on human health, ecosystems, and climate. This combination can be achieved either by comparing or complementing the techniques: the results of the comparison will allow to reduce the uncertainty of aerosol measurements in the atmosphere, with a subsequent improvement of model predictions on climate change, whereas the complementarity results in the possibility of investigating the aerosol from the ground up to the stratosphere. The new aerosol in-situ facility at CIAO, funded by the Italian Ministry of University and Research through the PER-ACTRIS-IT project (https://www.imaa.cnr.it/en/projects/38-attivita/progetti/713-per-actris-it, last access: 6 December 2023), has received initial acceptance as ACTRIS National Facility observational platform for the measurements of at least the obligatory ACTRIS aerosol in-situ variables. The site will start the next phase of the labelling process in 2024.

In this paper we present a concise overview of the observatory, focusing on the characteristics of the recently established ACTRIS-compliant in-situ facility, with the main aim to benefit the aerosol community providing a comprehensive and detailed description of technical solutions for the implementation of such component. After a short description of CIAO and typical atmospheric conditions in Sect. 2, Sect. 3 reports about the remote sensing instrumentation currently operating at CIAO. Section 4 represents the core of this paper, providing the in-depth description of the in-situ facility with the detailed configuration of each instrument and sampling lines. Finally, Sect. 5 illustrates three scientific topics to be studied at CIAO with the synergistic deployment of aerosol in-situ and remote sensing measurements.

https://doi.org/10.5194/amt-2024-57
Preprint. Discussion started: 13 May 2024

2 Description of the site

Equipped with state-of-the-art systems for remote-sensing and in-situ measurements of aerosol, CIAO (https://ciao.imaa.cnr.it, last access: 4 December 2023) is currently a reference observatory for atmospheric research in Europe. The site is located on the Southern Apennine in Italy (Tito Scalo, 40.60° N, 15.72° E, 760 m a.s.l.), in a plain surrounded by low mountains, less than 150 km away from the West, South and East coasts (Fig. 1).

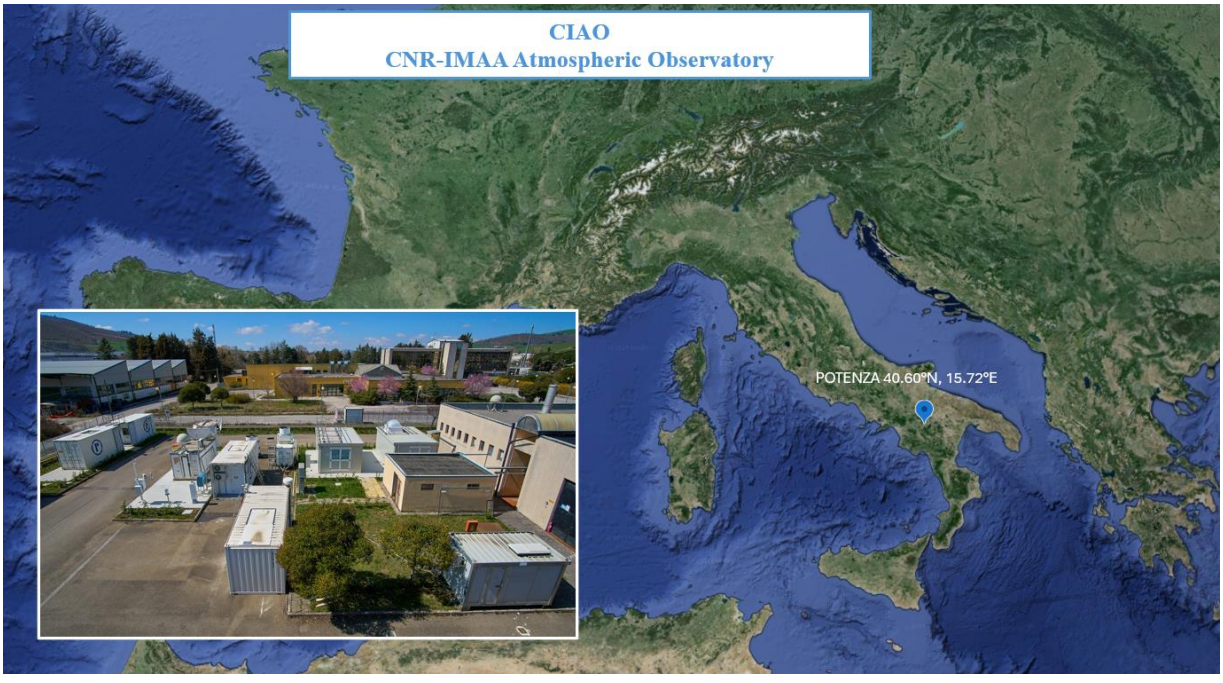

Figure 1: Location and image of CNR-IMAA Atmospheric Observatory (© Google Earth)

Therefore, it operates in a typical mountainous weather strongly influenced by Mediterranean atmospheric circulation, resulting in generally dry, hot summers and cold winters. Indeed, dew point temperatures at the station between 2018 and 2021 after sunset exceeded 15 °C only during summer (Fig. 2). The prevailing wind direction occurring at the site is W-WSW-SW (Fig. 3).

https://doi.org/10.5194/amt-2024-57
Preprint. Discussion started: 13 May 2024

Atmospheric Measurement Techniques Discussions

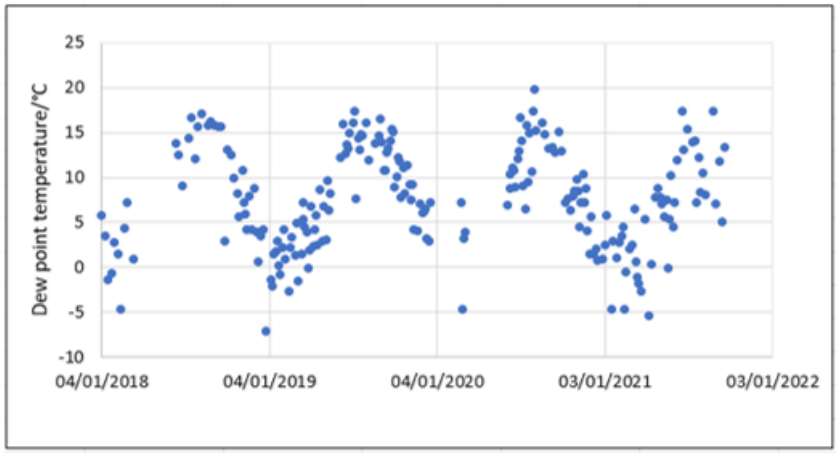

Figure 2: Dew point temperature time series at CIAO in the timeframe 2018-2021 calculated from the RH and temperature values measured at the ground level with the sensors of VAISALA RS41 radiosondes, typically launched twice a week between 30 and 120 minutes after sunset.

Most of the surrounding land is classified as arable crops in non-irrigated areas, followed by broad-leaved woods and coniferous forests, sclerophyllous or wooded/shrubby areas and natural grazing areas and grasslands (http://rsdi.regione.basilicata.it, last access: 28 November 2023).

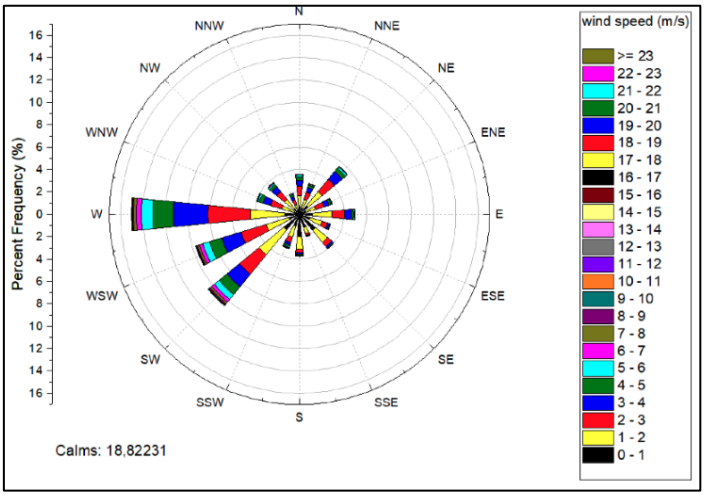

Figure 3: Wind rose diagram at CIAO in 2004-2017 obtained from continuous measurements of the automatic weather station VAISALA MILOS520 with temporal resolution of 1 minute.

CIAO's mission is to improve the knowledge of atmospheric processes and their role in meteorological phenomena, climate change and air quality. Given the coverage and global relevance of the processes studied, fundamental aspects of the activities

https://doi.org/10.5194/amt-2024-57
Preprint. Discussion started: 13 May 2024


Atmospheric Measurement Techniques Discussions

and approaches adopted are the development of internationally recognized Standard Operating Procedures, the open data policy and the full sharing of methodologies and know-how.

CIAO provides free and open access to national and international users like researchers, Small and medium-sized enterprises (SMEs), students and citizens. At the present time, CIAO extends its outreach through the ATMO-ACCESS Trans-National Access program (https://www.atmo-access.eu/second-call-for-access/, last access: 2 December 2023). This program allows participants to engage in research on aerosols and their effects, to learn techniques and methods, and to contribute to instruments, or to collaborate with the team.

The research activities of CIAO revolve around the long-term observations of aerosols, clouds, trace gases and greenhouse gases within the European research infrastructures ACTRIS and ICOS (Integrated Carbon Observing System), as well as around the participation of CIAO in reference observational programs and networks on a global scale, such as GRUAN (GCOS Reference Upper-Air Network) and GALION (GAW Aerosol Lidar Observation Network). The observational strategy is organized to provide quality assured measurements for satellite validation and model evaluation and to fully exploit the synergy and integration of the active and passive sensors for the improvement of the atmospheric characterization (e.g., Pappalardo et al., 2004;; Mona et al., 2009; Boselli et al., 2012; Ilić et al., 2022). The complete list of CIAO publications is available at https://ciao.imaa.cnr.it/publications/.

For what concerns aerosol measurements, CIAO due to its geographical position as well as the low aerosol background concentration is interesting for studying particles of natural origin such as desert dust and volcanic ash clouds. The site is regularly affected by Saharan dust intrusions (e.g., Mona et al., 2006; Mona et al., 2014; Binietoglou et al., 2015; Soupiona et al., 2020) has been reached by volcanic aerosol at the level of free troposphere during the eruptions of Etna (e.g., Pappalardo et al., 2004a, Villani et al., 2006) and Eyjafjallajökull (Madonna et al., 2010; Mona et al., 2012; Pappalardo et al., 2013) volcanos in 2002 and 2010, respectively, and stratospheric layers (e.g., Sawamura et al., 2012). In recent years, the observatory has become actively involved in the study of smokes originated by wildfires occurring both at short-range, spreading with increased frequency in the surrounding forestry areas during the summer period (De Rosa et al., 2022), and long-range transported plumes, such as the autumn 2020 California wildfires whose smokes transported in the stratosphere reached the site within 13 days (Baars et al., 2019).

3 Remote sensing measurements

Remote sensing measurements have been the backbone of the research activity at CIAO since its beginning in the early 2000s, with the scientific goal of providing long-term measurements for the climatology of aerosol and cloud properties. The main research lines currently include: a) development of advanced lidar systems for the study of aerosols and aerosol-cloud interactions; b) design and implementation of new products (such as aerosol typing, aviation-specific products, and atmospheric boundary layer height); c) development and implementation of open data and FAIR data management policies within the ARES node of the ACTRIS Data Center and RIs in the environmental field; d) development and implementation of

https://doi.org/10.5194/amt-2024-57
Preprint. Discussion started: 13 May 2024


Atmospheric Measurement Techniques Discussions

access policies to European RIs; e) deep/machine learning and signal processing applied to Earth observation; f) studies integrated with transport models, satellite data and climate models; g) harmonization of the time series of measurements of atmospheric variables; h) measurement campaigns for validation and integration with satellite data; i) networking at European and global level.

Besides the compliance to the ACTRIS guidelines, all the remote-sensing measurements performed at CIAO are designed to be in line with the main ground-based observation networks (i.e., EARLINET, CloudNet, AERONET, GRUAN, GALION) and the major international standards provided by the WMO/GAW 2016, aiming at establishing a long-term, harmonised and statistically significant database of measurements for climatological studies (Matthias et al., 2004).

The active remote-sensing instruments operative at CIAO include multi-wavelength Raman and polarization lidars, ceilometers, Doppler lidars and polarimetric Doppler radars, and the passive ones include microwave radiometers, photometers, and a high-resolution Fourier-Transform Infrared (FTIR) spectrometer.

With respect to the status of CIAO reported in previous papers (e.g., Madonna et al., 2011), some instruments are still operating, some have been replaced by more recent and advanced ones, and new instruments for increasing the observational capabilities have been added. The complete list of the remote sensing suite is reported in Table 1.

Aerosol Remote Sensing	Cloud Remote Sensing	Trace gases Remote Sensing
Fixed multi-wavelength Raman lidar	Ka-band Doppler radar Metek MIRA-35	FTIR Bruker 125HR
Mobile multi-wavelength Raman lidar	Compact Ka-band Doppler radar MIRA 35C	
Lidar and optical laboratories	W-band Doppler radar RPG-FMCW-94	
	K-band Doppler radar Metek MRR-PRO	
MUSA Transportable Fixed multi-wavelength Raman lidar	Microwave radiometer RPG-HATPRO-G5	
Scanning UV Raman lidar	Ceilometer Vaisala CL51	
Automatic sun/sky/lunar photometer Cimel 318T	Ceilometer Vaisala CL31	
	Ceilometer Lufft CHM15k	
	2 Doppler lidars Halo Photonics Stream LineXR	

Table 1: List of the CIAO Remote Sensing instruments

For the aerosol remote sensing, two new highly-advanced lidar systems have been recently installed at CIAO, one fixed and one mobile. The first one will be an ACTRIS Observational Platform and the second one an Exploratory Platform available even in combination with cloud remote sensing equipment. Both the lidars are capable of carrying out continuous measurements going well beyond the required ACTRIS/EARLINET standards. They are able to provide measurements of vertical profiles of several aerosol optical properties: backscatter coefficient and particle depolarization at 1064, 532 and 355 nm, and extinction coefficient at 532 and 355 nm, with the observational range starting from 200m up to at least 20km of altitude. The fixed lidar is able to reach a measurement altitude range higher than 20km, being equipped with two telescopes,

https://doi.org/10.5194/amt-2024-57
Preprint. Discussion started: 13 May 2024


Atmospheric Measurement Techniques Discussions

and to provide vertical profiles of water vapor mixing ratio, this latter useful for investigating the impact of water vapour on aerosol properties. On the other hand, the mobile system is more compact and transportable, and is used for field campaigns. Both systems are part of the Centre for Aerosol Remote Sensing (CARS), one of the ACTRIS central facilities, that has the mission to offer operation support to ACTRIS National Facilities operating aerosol remote sensing instrumentation. The two systems are reference lidars for ACTRIS and offer services to test the performances of other lidar systems also through on-site direct intercomparison campaigns using the mobile lidar.

Close by to the aerosol multiwavelength depolarization Raman, a triple mode photometer is operational within AERONET (AErosol RObotic NETwork) and ACTRIS providing columnar aerosol optical depth measurements and columnar size distribution information not only in daytime, but also in night-time under certain illumination conditions. CIAO is also equipped with a lidar laboratory and an optical laboratory. The lidar laboratory is a facility that allows to implement and test several and customized lidar configurations (fluorescence, HSRL, multiwavelength elastic/Raman/depolarization and water vapour mixing ratio and liquid water, and rotational Raman for temperature) in a modular way. The optical laboratory allows to test and characterize optical components and laser sources typically used in high power lidar systems. Both laboratories are also part of CARS and are open to users who want to benefit from the offered services.

Besides the aerosol remote sensing instruments, cloud remote sensing equipment has also been updated and expanded with additional complementary instruments, setting up both an Observational Platform and a mobile Exploratory Platform compliant with ACTRIS/CloudNet requirements. Among the complementary instruments, Doppler lidars are capable of measuring the profiles of horizontal and vertical wind and related fluid dynamic parameters through the troposphere. Finally, a high resolution FTIR spectrometer has been added for performing remote sensing measurements of trace gases to complement the other observations.

The availability of a large number of remote-sensing systems at the observatory has enabled the possibility to both compare and combine different techniques for studying atmospheric parameters. The synergy between lidars and photometer observations allows the retrieval of vertical profiles of aerosol concentration for total, fine and coarse components through algorithms like GARRLiC (Generalised Aerosol Retrieval from Radiometer and Lidar Combined data; Lopatin et al., 2013) and POLIPHON (Polarization Lidar Photometer Networking; Mamouri and Ansmann, 2016; 2017). Ceilometers have shown good capabilities in the detection of aerosol plumes even if with some limitations (Wiegner et al., 2014; Madonna et al., 2015). The combined use of ceilometers and multiwavelength polarization Raman lidars can be an added value for aerosol variability investigation. Additional cloud information provided by 24-h ceilometers can be precious for cloud masking prior to the analysis of lidar measurements for aerosol profiling. These aspects are currently under investigation and developments within ACTRIS implementation.

The combination of lidars and radars also demonstrated the enhancing power of synergistic observations: combination of lidar and radar measurements during the Iceland volcanic eruption in 2010 showed radar capability of detecting giant volcanic particles (Madonna et al., 2010; Madonna et al., 2013).

https://doi.org/10.5194/amt-2024-57
Preprint. Discussion started: 13 May 2024

Atmospheric Measurement Techniques Discussions

Synergistic approach has been proposed for the study of thin liquid water clouds, combining multi-wavelength lidar and Doppler radar measurements (Rosoldi et al., 2022). It has been shown that microwave radiometer can be used to calibrate Raman lidar measurements for water vapour profiling and that the synergy between these instruments is an effective means for atmospheric water vapour monitoring (Madonna et al., 2006, Mona et al., 2007).

However, despite its huge potential in atmospheric research, there are two major drawbacks associated with the remote sensing observations: the inability to conduct aerosol measurements under skies with low clouds and precipitations, along with the impossibility of characterising the particulate properties near the ground. Therefore, the recent implementation of the in-situ facility described in the next section is fundamental to achieve a complete characterization of the aerosol at the ground level where the aerosol particles directly affect ecosystems and human health. In addition, the in-situ measurements include the valuable chemical characterization of the particulate matter (PM), thus providing a deeper comprehension of the aerosol type, the source apportionment and the mixing atmospheric processes.

4 Description of the aerosol in-situ facility

4.1 Overview

The in-situ facility recently installed at CIAO comprises two main parts (Fig. 4): a field laboratory for aerosol online measurements with continuous instrumentation and PM samplers and a chemical laboratory for the post-sampling analysis of particulate collected over the filters.

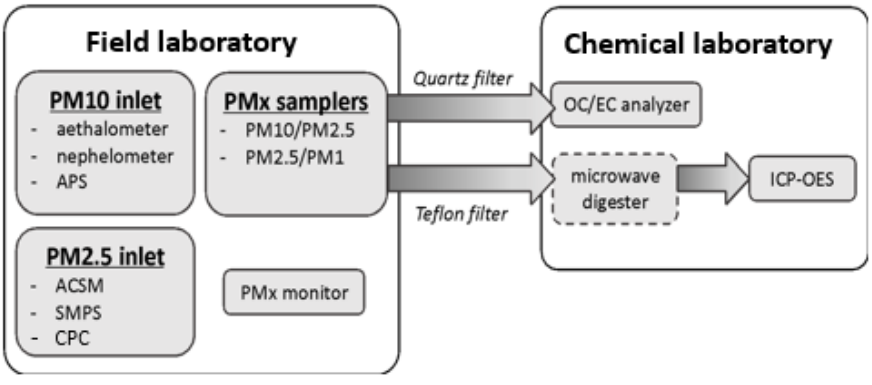

Figure 4: Outline and workflow of the in-situ facility at CIAO.

The shelter has been designed according to the ACTRIS guidelines and recommendations (Wiedensohler et al., 2014), with the instrumentation arranged as follows: a dual spot aethalometer (AE33, Magee Scientific), a multi-wavelength integrating

https://doi.org/10.5194/amt-2024-57
Preprint. Discussion started: 13 May 2024

Atmospheric Measurement Techniques Discussions

nephelometer (AURORA 3000, Ecotech) and an aerodynamic particle sizer (APS 3321, TSI) located under a common PM_{10} (aerosol particles with an aerodynamic diameter less than 10 μm) inlet; a time-of-flight aerosol chemical speciation monitor (ToF-ACSM, Aerodyne Research), a scanning mobility particle sizer (SMPS, 3938-TSI) and a condensation particle counter (CPC, 3750-TSI) placed under a $PM_{2.5}$ (aerosol particles with an aerodynamic diameter less 2.5 μm) common inlet. Additionally, two PMx samplers (SWAM 5a-Dual Channel Monitors, FAI Instruments) and a PMx monitor (EDM 180, Grimm) are placed as standalone instruments with individual sampling lines.

Particular attention has been devoted to the design of the common inlets and the sampling lines. The PM_{10} and $PM_{2.5}$ common impactor type inlets, operating at a flow rate of 16.7 l min^{-1}, are compliant with EN 12341 and EN 14907 standards, respectively. The main challenge when transporting aerosol to collectors and aerosol measuring instrumentation is to avoid aerosol losses. Therefore, firstly, the internal diameter of the main sampling pipe of the common PM_{10} and $PM_{2.5}$ inlets must be such as to ensure that the sampled air has a laminar flow along the entire path (Reynolds number less than 2000) to minimise the loss of particles by diffusion and inertia. The instrument sublines (characterised by smaller inside diameters) are connected to the common inlet through an isokinetic flow splitter where the sample flow velocity is almost equal to the velocity of the main flow. Moreover, the ends of the tube in the isokinetic flow splitter must be sharp to ensure a homogeneous distribution of the air sample to the instruments. Another key feature of the splitter is that the sample is collected from the core of the main aerosol flow rather than from streamlines near the wall of the main pipe, therefore, ensuring a representative sampling (especially for coarse and nanoparticles).

The technical details of the common inlets and isokinetic splitters are shown in Table 2.

Common Inlet					**Isokinetic splitter**				
Inlet	**Flow rate ($l\ min^{-1}$)**	**Int. Diameter (mm)**	**Speed ($m\ s^{-1}$)**	**Reynolds Number**	**Instrument**	**Int. Diameter (mm)**	**Flow rate ($l\ min^{-1}$)**	**Reynolds Number**	**Speed ($m\ s^{-1}$)**
PM 10	16.7	21.2	0.8	1135	Aethalometer	8	3	885	1.6
					Nephelometer	8	5	885	1.6
					APS	4.4	1	320	1.09
	16.7	21.2	0.8	1135	SMPS	4.4	2	655	2.2
					CPC				

https://doi.org/10.5194/amt-2024-57
Preprint. Discussion started: 13 May 2024

PM 2.5					TOF-ACSM	8	3	530	1

Table 2: Technical details of the common inlets and isokinetic splitters.

All the sampling tubes are kept as short as possible and are placed in vertical position with bends and connectors avoided as much as possible to suppress potential sources of turbulence, which would result in additional losses of particles. In addition, the tubes are made of polyurethane antistatic material to guarantee perfect dissipation of accumulated static electricity, because the static charges may remove significant portions of the aerosol to be sampled. The inlets on the rooftop of the field laboratory are placed at one metre from each other and height of 1.5-2.0 m above the roof with the aim of minimising local influences and potential interferences in the sampling process.

In compliance with the ACTRIS indications, all the instruments in the laboratory are equipped with a Nafion dryer tube which keeps the RH well below 40%; under this threshold, in fact, changes in particle diameter due to RH variations are expected to be lower than 5%, thus obtaining comparable data, independent of the hygroscopic behaviour of the aerosol particles. Moreover, the upstream drying prevents the possible instrument damage caused by water condensation.
The Nafion dryers of Aethalometer, Nephelometer, APS and ACSM operate in a reflux mode, shown in Fig. 5, which returns the dry sample back to the dryer for use as the purge after it has gone through the analyzer. Since this method uses all the dry sample as purge air, only the sample flow required for analysis passes through the dryer. This results in a high drying efficiency. The vacuum on the purge air should be at least 15 inches Hg, with a higher vacuum preferable. This vacuum level is required to provide the desired 2:1 purge to sample flow ratio based on the actual volumetric flow.

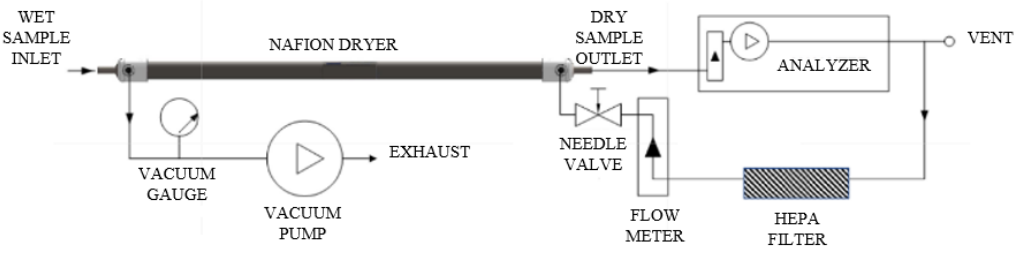

Figure 5: Schematic Diagram - Nafion Reflux mode (MD-700-User-Manual, https://www.permapure.com).

Instead, the Nafion dryer connected to the SMPS and CPC, since the instruments need n-butanol as a working liquid for the growth of aerosol particles, cannot operate in reflux mode but operates in counter flows using air dry coming from a compressor (Acoem 8301 LC-H Zero Air Generator) (Figure 6).

https://doi.org/10.5194/amt-2024-57
Preprint. Discussion started: 13 May 2024

Atmospheric Measurement Techniques Discussions

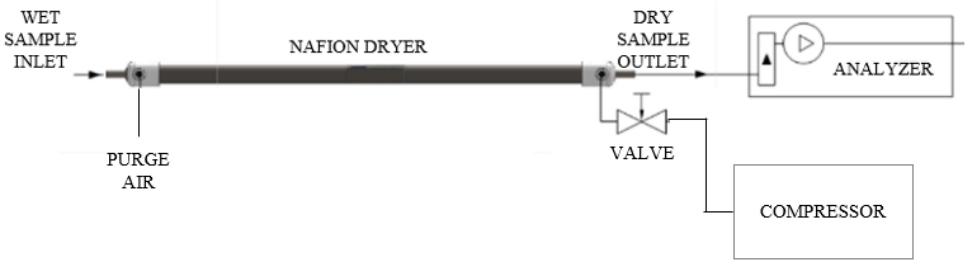

Figure 6: Schematic Diagram - Nafion counter flows mode.

Moreover, at the input of each instrument, there is a high-resolution sensor connected to a software for continuous monitoring (every minute) of relative humidity and temperature. The accuracy of the sensors is 2.5% for the RH and 0.5°C for the temperature.

Lastly, in order to limit the temperature variation around the instruments, a continuously operating air conditioning system set at 23 °C has been installed in the laboratory.

As previously mentioned, the in-situ facility is complemented by the chemical laboratory which enables complementary measurements on the particulate-loaded filters coming from the PMx samplers, that is not possible to obtain with the continuous instrumentation. The chemical laboratory include: an inductively coupled plasma optical emission spectrophotometer (ICP-OES, series 5800, Agilent) used to perform the analysis of trace metals, and a multi-wavelength OC/EC analyzer (DRI model 2015, Magee Scientific) used to analyse the carbonaceous fraction of the collected particulate.

4.2 Instrumentation under the common PM_{10} inlet

As reported above, a PM_{10} common inlet is used to feed the aethalometer, the nephelometer and the APS. The aethalometer is a key instrument for wildfire and pollution characterization, being able of detecting the fraction of particulate which absorbs light, known as Black Carbon (BC), formed during the incomplete combustion of carbonaceous matter from biomass burning and fossil fuel (Petzold et al., 2013). According to the ACTRIS guidelines, the AE33 aethalometer operating at seven different wavelengths in the range 370-950 nm is used for the real-time monitoring of the concentration of BC. Briefly, the principle of the aethalometer is to measure at given time intervals the attenuation of a light beam (at 880 nm) transmitted through a filter where the particulate is continuously collected; the rate of change of optical transmission combined with the air flow rate monitored through a mass flowmeter permits to determine the absorption coefficient, then converted into BC concentration by means of the mass-absorption cross section. The dual spot technology refers to the contextual measurement of transmitted light intensities through two separate spots of the filter at different loading levels, thus allowing to compensate for the so-called loading effect largely described by Drinovec et al. (2015). The aethalometer is equipped with a sample stream dryer (Magee Scientific) exploiting a semi-permeable Nafion membrane which keeps the RH well below 40%.

https://doi.org/10.5194/amt-2024-57
Preprint. Discussion started: 13 May 2024


Atmospheric Measurement Techniques Discussions

Among the other in-situ instruments placed under the PM_{10} inlet, the nephelometer can be considered in a certain way complementary to a ground-based lidar, expecting therefore to provide optical parameters consistent with those obtained from the lidar within the atmospheric planetary boundary layer (PBL). However, when the the PBL is particularly shallow (e.g., during wintertime), the nephelometer becomes the only tool to obtain the optical parameters of the aerosols residing within the first hundreds of metres from the ground. The ACTRIS-compliant integrating nephelometer AURORA 3000 is used to measure the total scattering (σ_{sp}) and the backscattering (σ_{bsp}) coefficients (integrating within the angular range 9°-170° and 90°-170°, respectively), both correlated to the particle concentration (i.e., extensive properties). The peculiarity of the instrument is the utilisation of a light source emitting at three distinct wavelengths: the light at 635 nm (red) interacts strongly with large particulate matter such as desert dust and sea salt; the light at 525 nm (green) interacts strongly throughout the human range of visibility (smog, fog, haze); the light at 450 nm (blue) interacts strongly with fine and ultrafine particulates, such as wood fires and automobile combustion particulate. The nephelometer is equipped with a 36-inch-long Perma Pure Nafion MD-700 in order to prevent condensation of water droplets over the particles, which would increase their size and significantly change their scattering characteristics.

Lastly, the APS spectrometer provides high-resolution real-time aerodynamic measurements for the coarse fraction of the particulate (Peters et al., 2003). The optical size range of the APS is from 0.37 to 20 µm, but since the spectrometer is connected to a PM_{10} inlet and the counting efficiency of APS below 0.8 µm aerodynamic diameter rapidly decreases and is unstable, the realistically size range is from 0.8 to 10 µm. The APS is based on the time-of-flight particle sizing, in which the aerodynamic size of a particle determines its rate of acceleration, with larger particles accelerating more slowly due to increased inertia; the time of flight between two laser beams is recorded and converted to aerodynamic diameter using a calibration curve. The instrument measures in parallel the light scattering intensity of the sized particles in the equivalent optical size range from 0.8 to 10 µm, thus providing further insights into the aerosol nature and composition.

The APS is connected to the sampling line just with the inner nozzle (sampling 1 l min^{-1}) from the common sampling line and the flow is dried by a 12-inch Perma Pure Nafion, while taking the additional sheath flow (4 l min^{-1}) from the air compressor.

4.3 Instrumentation under the common $PM_{2.5}$ inlet

Even though the general ACTRIS recommendations for the in-situ measurements involve the analysis of the PM_{10} fraction, the CPC, the SMPS and the ACSM represent an exception and are more conveniently placed under the cut-off size of a $PM_{2.5}$ inlet. The ACTRIS-compliant CPC is used to measure the number concentration of aerosol particles with diameter > 10 nm. In the CPC, an aerosol sample is continuously drawn through a heated saturator where the butanol is vaporized and diffused into the sample stream. Together, the aerosol sample and *n*-butanol vapour pass into a cooled condenser where the *n*-butanol vapour becomes supersaturated and condenses on the particle surface causing them to grow. The particles are then counted individually as they pass through a laser-based optical detector.

Regarding the SMPS, it is an instrument of interest for CIAO, being able to provide the size distribution and concentration of the fine fraction of the particulate in the size range 10 nm – 800 nm. It consists of four components in sequence: 1) a pre-

https://doi.org/10.5194/amt-2024-57
Preprint. Discussion started: 13 May 2024


Atmospheric Measurement Techniques Discussions

impactor which removes particles larger than the fixed upper limit of size; 2) a bipolar diffusion charger (model 3082, TSI) which confers a characteristic stationary charge distribution to the polydisperse particles by using a radioactive source (Kr-85); 3) a differential mobility analyzer column (DMA, model 3083, TSI) which separates the particles according to their electrical mobility by varying continuously the applied voltage within the column (Schmid et al., 2007); and 4) a condensation particle counter (CPC, model 3750, TSI) where the classified monodisperse particles are counted after condensation of *n*-butanol on their surface.

The CPC and the SMPS are connected to the same 24-inch Perma Pure Nafion via a T-flow splitter in order to keep the RH below 40%. Moreover, a dry sheath air is needed for the SMPS to ensure particle sizing inside the DMA with a minimum fluctuation in RH and for this purpose a Silica Dryer Tube (model 3082, TSI) is incorporated in the DMA sheath flow system, which is a closed loop.

For what concerns the aerosol mass spectrometry techniques, the ToF-ACSM (Aerodyne Research) has been shown to be perfectly suited for the ACTRIS observatory platforms, having been designed to provide continuous and unattended measurements for aerosol monitoring on the timescale of years. The chemical speciation with high temporal resolution is a unique feature of the ACSM technology, unobtainable with conventional filter sampling and subsequent post-processing chemical methods; moreover, the ACSM is not subjected to sampling artefacts that affect the collection of semi-volatile PM components by means of filters (Viana et al., 2006; Kim et al., 2015). The ToF-ACSM chosen for CIAO was introduced in 2013 (Fröhlich et al., 2013), providing a higher mass resolution (i.e., $m/\Delta m$ = 600) and superior detection limits (i.e., < ng m^{-3}) with respect to the previously developed quadrupole-ACSM (Ng et al., 2011) for a time resolution of 30 min. The instrument measures the mass and chemical composition of non-refractory submicron aerosol particles – i.e., organic substances, nitrates, sulphates, ammonium, and chloride – thus generating an invaluable database for the research community to characterise the particulate sources and evolution. The operational principle of the instrument is briefly described in the following: the aerosol enters the inlet where the aerodynamic lens efficiently samples and focuses submicron particles to the subsequent vacuum chamber; here, the particles impact on a resistively heated porous tungsten surface at approximately 600 °C which vaporises the non-refractory particulate; the vaporised matter is subsequently ionised by electronic impact and detected through the ToF analyzer. In this case, the 24-inch Nafion dryer installed upstream the instrument eliminates the complicating inlet effects due to particle composition dependent water uptake (Middlebrook et al., 2012).

ACSM was installed in February 2023 and worked for some months in almost continuous way. Then some interventions were requested to accomplishing the optimization requests from ACTRIS aerosol in situ central facility, and the ACSM restarted operations just recently in April 2024. Anyhow the 3 months of almost continuous measurements performed in 2023 already provide some insights about aerosol present at the surface in Potenza. Figure 7 reports daily concentrations for the 4 components as measured by ACMS in February-March-April 2023 period. Median values are preferred to mean ones for avoiding the strong influence of outliers and spikes in the reported values. Monthly pie charts show the relevance of the difference components for each one of the 3 months. As a general comment, we could say that the Potenza site is clearly a rural site with low PM concentration and a very high contribution of the organic substances (see for comparison as example

https://doi.org/10.5194/amt-2024-57
Preprint. Discussion started: 13 May 2024

Atmospheric Measurement Techniques Discussions

Atabakhsh et al., 2023 and Zhao et al., 2020). The observed increasing in the total concentration but more pronounced in the organic component could be related to tree pollen events typically occurring in such period.

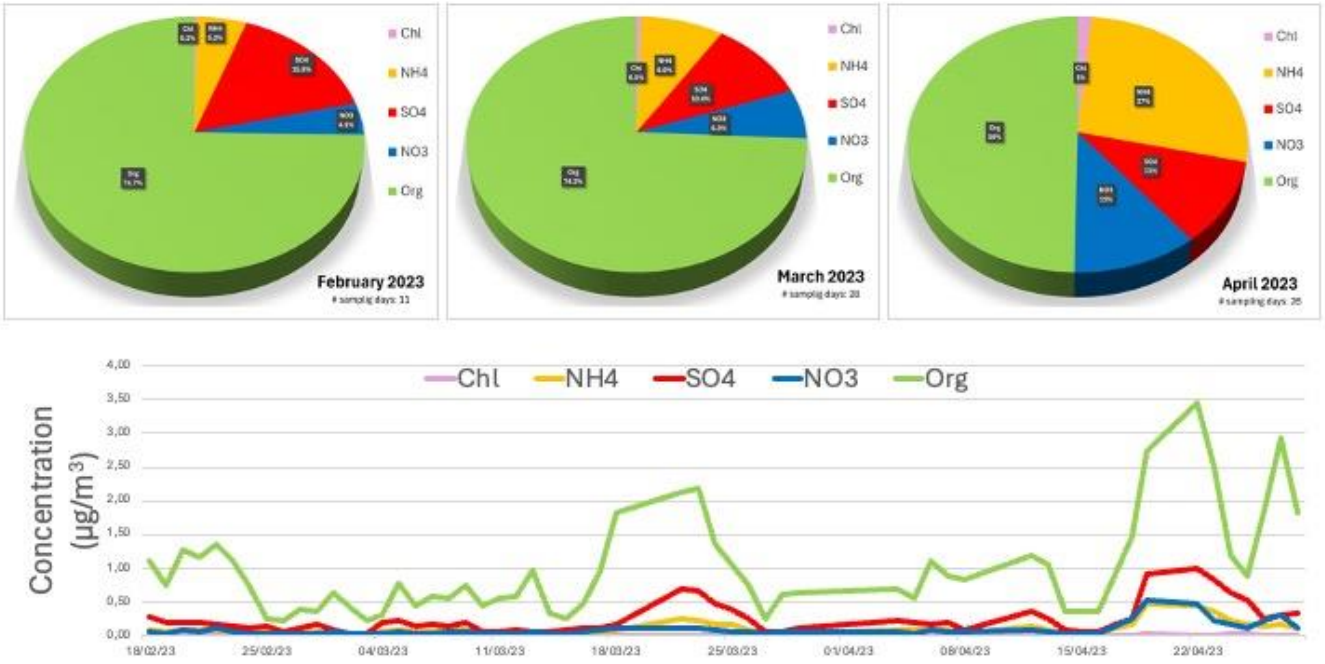

Figure 7: Daily medians of the mass concentration and mass fraction of each of the 4 chemical components of non-refractory submicron aerosol particles observed at CIAO in February – March – April 2023.

4.4 PMx samplers and PMx monitor

Additionally to the online instruments report above, the field laboratory is equipped with two PMx samplers for the continuous sampling and concentration measurement of PM_{10}, $PM_{2.5}$ and PM_1 (aerosol particles with an aerodynamic diameter less than 1 µm) mass fractions collected over both Teflon and quartz filters; the determination of the mass of collected samples is based on the β-ray attenuation equivalent method, which strongly reduces the workload and the operator-associated variability if compared to the standard gravimetric method (Baltensperger et al., 2001). In particular, the device measures the attenuation of β-ray across the filter medium which collects particulate matter, and the attenuation of intensity in β-ray is proportional to the amount of material present. Each PMx sampler is equipped with two independent sampling lines (i.e., $PM_{10}/PM_{2.5}$ and $PM_{2.5}/PM_1$), thus enabling the simultaneous collection of different PM fractions on independent filters. According to the workflow reported in Fig. 4, the particulate collected over the filters is subjected to further analysis within the chemical laboratory: the PM_{10}, $PM_{2.5}$ and PM_1 collected over 24h on Teflon filters are analysed to determine the concentration of metals

https://doi.org/10.5194/amt-2024-57
Preprint. Discussion started: 13 May 2024


Atmospheric Measurement Techniques Discussions

by means of the ICP-OES. On the other hand, the $PM_{2.5}$ collected over 24h on quartz fibre filters are analysed to quantify the organic carbon (OC) and elemental carbon (EC) fractions using the thermal optical method by the OC/EC analyzer; the utilisation of quartz fibre filters for the OC/EC analysis is strictly recommended by the WMO/GAW 2016 guidelines, and it constitutes the only exception to the Teflon filters commonly used for other analyses. In fact, the particulate collected on Teflon filters is not limited to ICP-OES analysis but can also be analyzed through alternative techniques such as X-ray fluorescence (XRF) and Particle Induced X-ray Emission (PIXE) in order to find complementarities between the three techniques for the determination of a range of metals.

Furthermore, even if not included in the mandatory ACTRIS variables to be measured, the mass concentration for the cut-off diameters of PM_{10}, $PM_{2.5}$ and PM_1 belongs to the set of standard measurements to monitor the particulate matter, providing insight into the separation of fine and coarse particles within the aerosol.

The PMx monitor operating at CIAO currently represents one of the main automated measurement systems for studying the concentration levels of particulate matter in ambient air. Based on the detection principle of the light scattering at the level of single particles, the system offers simultaneous real-time measurements of PM_{10}, $PM_{2.5}$ and PM_1 and particle number distribution with a resolution of 0.1 $\mu g\ m^{-3}$.

4.5 Chemical laboratory

The CIAO chemical laboratory is equipped with an ICP-OES and an OC/EC analyzer. The ICP-OES (5800 series, Agilent) is used to determine the qualitative and quantitative elemental composition of the metals present in the atmospheric particulate with high sensitivity, at values below the 1 $\mu g\ l^{-1}$ limit for certain elements. The metals are introduced into the atmosphere from various anthropogenic and natural sources. Anthropogenic metals are released into the atmosphere during combustion of fossil fuels and wood, as well as during high temperature industrial processes and waste incineration; natural emissions result from a variety of processes acting on crustal minerals, including volcanism, erosion, surface winds, forest fires and ocean evaporation (Allen et al., 2001; Pakkanen et al., 2001; Rajšić et al., 2008). Various metals are used as marker for the identification of emission sources: aluminium and silicon are primarily derived from soil and rocks (crustal elements); sodium and chlorine are typically associated to marine aerosols; arsenic, cadmium, manganese and lead mostly derive from combustion of fossil fuels occurring at high temperature, to name a few. The ICP-OES analysis of particulate matter requires a preliminary microwave digestion of the filter in acidic conditions to extract the metals, carried out by means of a microwave digester (ETHOS UP, FKV). The obtained liquid sample is then nebulized and introduced into the plasma as an aerosol suspended in the argon gas: due to the high temperatures within the plasma (7000 – 10000 K), a significant fraction of most elements exists as atoms or ions in the excited state, causing an intense polychromatic emission which continuously brings back the elements to their ground state. The polychromatic emitted light is dispersed into individual wavelengths by a polychromator and detected by a photosensitive charge-coupled device (CCD). The concentration of each metal in the sample is obtained by using a calibration curve referred to a solution containing the analysed elements of known concentration.

https://doi.org/10.5194/amt-2024-57
Preprint. Discussion started: 13 May 2024


Atmospheric Measurement Techniques Discussions

The multi-wavelength OC/EC analyzer (2015 DRI, Magee Scientific) compliant with ACTRIS is used to quantify the total carbonaceous content of the particulate matter (total carbon, TC) and the OC and EC subfractions. EC is essentially a primary pollutant, emitted directly from the incomplete combustion of fossil fuels and the pyrolysis of biological material during combustion, whereas OC can be directly emitted from the incomplete combustion of organic materials and the degradation of carbon containing products such as vegetation – primary OC – or produced from atmospheric reactions, involving gaseous organic precursors, i.e., secondary OC (Zhou et al., 2006). The operational principle of the thermal/optical analysis is based on the preferential desorption of OC and EC materials under different temperatures and atmospheres programmed within specific thermal protocol, such as the EUSAAR_2 (Cavalli et al., 2010) which is currently used within the ACTRIS community. OC usually desorbs under a non-oxidising helium atmosphere at temperatures up to 570 °C, while the EC is combusted in an oxidising atmosphere with 2% O_2 at temperatures up to 850 °C. However, since part of the OC turns into the light-absorbing pyrolytic carbon which desorbs during the oxidising mode, the correct discrimination between the OC and the EC fractions is conveniently identified with the point at which the light transmission reaches the pre-pyrolysis value. The liberated carbon is then completely oxidised to carbon dioxide passing through a heated catalyst MnO_2 and finally quantified by an NDIR detector.

5 Synergistic deployment of aerosol remote sensing and in-situ measurements

Synergistic approaches combining aerosol profiling and in-situ measurements are one of the most beneficial strategies in aerosol research, allowing an accurate typing and estimation of the impacts of particulate matter (Molero et al., 2020). Remote sensing techniques provide the vertical profile of the particle size distribution of the aerosol as well as further physical and optical properties useful for understanding complex atmospheric phenomena (Vratolis et al., 2020); however, they are not able to provide information under cloudy sky conditions or at the ground level, where the identification of aerosol type is only possible using the in-situ instrumentation. The in-depth typing of the aerosols requires the information on the chemical composition, attainable only by means of in-situ measurements. The complete set of data resulting from the combined approaches is crucial for identifying the sources and the evolution of concentration levels of particulate matter over time (Bressi et al., 2021), and it is of paramount importance for the implementation of controls or policies to reduce aerosols that negatively affect air quality and public health.

The complete picture of the aerosol-typing is also expected to clarify further the climate effects of particulate matter. In fact, the estimation of the radiative effect of atmospheric aerosol requires the knowledge of multiple parameters, including the aerosol load, the optical properties, the chemical composition, the presence of clouds and the albedo of the underlying surface. The accurate identification of aerosol types is also needed to improve the understanding of atmospheric dynamics and long-range transport, to improve satellite aerosol retrieval algorithms, and to validate climate models.

The multiwavelength polarisation Raman lidar is a well-established active remote sensing technique for the detection and characterization of aerosol-types (Nicolae et al., 2018; Papagiannopoulos et al., 2018). Specifically, it can provide vertically

https://doi.org/10.5194/amt-2024-57
Preprint. Discussion started: 13 May 2024


Atmospheric Measurement Techniques Discussions

resolved information on extensive (e.g., aerosol backscatter coefficient, aerosol extinction coefficient and volume depolarization ratio) and intensive (e.g., Ångström exponent, lidar ratio and particle depolarization ratio) aerosol optical properties. The extensive properties depend on the aerosol concentration, whilst intensive ones are type-sensitive providing indication about the particle size, shape, and indices of refraction that allow for the characterization of different aerosol types. Nevertheless, the intensive properties might not be sufficient to guarantee accurate typing, as some aerosol types (e.g., volcanic and desert dust particles) have very similar intensive properties but are attributed to different sources and generating mechanisms. For this reason, the discrimination of aerosol particles that typically have the same optical characteristics calls for the combined use of lidar observations and transport model simulations.

Finally, the aerosol in-situ observations can help in the assessment of the uncertainty of remote sensing-retrieved products like mass concentration, refractive index and fine-particle concentration obtained through inversion algorithms (e.g., Veselovskii et al., 2012; Lopatin et al., 2013).

In the following subsections we present three emblematic cases recurring at CIAO where the combined deployment of the in-situ and remote sensing observations is expected to be of added value: 1) Wildfires become more and more relevant in the Mediterranean, especially in view of the changing climate that is expected to increase temperature and in turn will affect their frequency, duration and intensity in the next decades. In this context, small and local fires are widely distributed and their characteristics and assessment could be important at global level. De Rosa et al. (2022) showed with the use of lidar observations that fresh fires can be surprisingly characterised by low absorption; this would imply a different impact of local fires in the radiation budget which requires investigation and validation by means of in-situ measurements. 2) Local pollution during winter and adverse weather can be investigated in a more exhaustive manner only by in-situ observations, since lidar observations provide very little information due to the generally low and unresolved by lidars PBL height. 3) Desert dust intrusions often reach Europe and especially the Mediterranean Basin affecting local air quality, health and ecosystem and socio-economic sectors (e.g., Monteiro et al., 2022). Given all the above, the deployment of in-situ measurements at well-equipped sites like CIAO is crucial to quantify the impact at the ground level.

5.1 Local wildfires

The study of smokes from wildfires spreading in short distance represents a great example for a synergistic approach based on remote-sensing and in-situ techniques. In such a case, the smoke particles spread mainly at low levels and deposit fast on the ground, where in-situ measurements are the only tool to provide reliable information to support and integrate what is observed above medium overlap region, a prerogative of remote-sensing techniques.

The multiwavelength polarisation Raman lidar is a well-known tool to study smoke layers in the atmosphere, being able to separate aerosols according to their specific optical signature (Ohneiser et al., 2021). Specifically, a sign of the dominance of smoke in the aerosol layer is the aerosol extinction-to-backscatter ratio (the so-called lidar ratio, S) at 532 and 355 nm, which is typically high (i.e., > 50 sr) as a consequence of the presence of absorbing BC produced during the biomass burning;

https://doi.org/10.5194/amt-2024-57
Preprint. Discussion started: 13 May 2024


Atmospheric Measurement Techniques Discussions

moreover, the ratio of S measured at the different wavelengths may be used as an indicator of the phase of the ongoing wildfire (e.g., Nicolae et al., 2013). Other lidar parameters largely used to investigate the smoke are the particle linear depolarization ratio (PLDR) and the Ångström exponent (AE), which provide information about the shape and the size of the particles, respectively. In the case of a local wildfire, the observation of quasi-spherical and relatively small particles is expected, since the newly produced smoke particles do not have the time to undergo modifications during transport.

The Ångström absorption and scattering exponents (AAE and SAE) - derived from the aethalometer and nephelometer measurements, respectively - provide the optical typing of the smoke, with the value of AAE expected to correlate with the lidar observations (Cazorla et al., 2013) and, therefore, to the nature of spreading fire.

Among the aerosol in-situ instruments, the aethalometer is crucial to study smokes produced during wildfires, being able to quantify the BC originated from the incomplete combustion of carbonaceous matter and providing an estimate of the biomass burning (BB) apportionment to the overall BC (Sandradewi et al., 2008). Furthermore, particles resulting from the incomplete combustion have been reported to contain a significant organic carbon fraction, including numerous known toxic and carcinogenic polycyclic aromatic hydrocarbons (PAHs) (Nelson et al., 2021). To access relative amounts of organic carbon, the method involves comparing two optical indicators of carbonaceous particulate matter derived from the aethalometer measurements: BC at 880 nm, measuring elemental carbon that absorbs a broad spectrum of wavelengths, and UVPM at 370 nm, measuring particulate matter that, due to increased organic carbon content, absorbs disproportionately in the UV range compared to BC (Olson et al., 2015), UVPM, also known as brown carbon, is associated with toxic species such as PAHs and has been observed to be elevated in smoke resulting from biomass burning (Huangh et al., 2018). Additionally, the OC/EC thermal/optical analysis on $PM_{2.5}$ fraction is very important because the increase of organic carbon and elemental carbon concentrations has been the most indicated as an element that reflects wildfire emissions. The fine particles, particles generally 2.5 µm in diameter or smaller, represent a main pollutant emitted from wildfire smoke so other important in-situ analyses of the travelled smoke are the size distribution and concentration of fine particles by the SMPS and CPC, respectively. In fact, it is expected that the fine mode will be more densely populated and concentrated during these events compared to the rest of the year. Further confirmation of the increase in fine and ultrafine particulate matter during fire events is given by the $PM_{2.5}/PM_{10}$ and $PM_1/PM_{2.5}$ ratios obtained from the real-time measurement of PM_{10}, $PM_{2.5}$ and PM_1 concentrations using the PMx monitor. In fact, the mean fraction of fine PM ($PM_{2.5}/PM_{10}$) and ultrafine PM ($PM_1/PM_{2.5}$) is expected to be significantly higher during the fire period compared to the non-fire period. Finally, the in-situ investigation of wildfire smoke is completed by the chemical analysis obtained with the ToF-ACSM: in particular, key tracers of biomass burning organic aerosol in mass spectra are the enhanced signals at m/z 60 and 73 Th attributed to $C_2H_4O_2^+$ and $C_3H_5O_2^+$ ions, respectively, coming from the fragmentation of the so-called “levoglucosan-like” species originated from the pyrolysis of cellulose (Cubison et al., 2011). Finally, the chemical analysis of the filters through the ICP-OES is fundamental for tracking the levels of potentially toxic elements (PTEs) such as As, Sb, Cd, Hg, Pb, Cr, Cu, Ni, Se, Tl, Sn, V, and Zn. This monitoring is vital as these elements have the potential to be released into the environment during wildfires, posing a threat to humans and animals when their absorbed doses surpass the established reference values (Pacifico et al., 2023).

https://doi.org/10.5194/amt-2024-57
Preprint. Discussion started: 13 May 2024


Atmospheric Measurement Techniques Discussions

5.2 Local pollution in wintertime

Winter months commonly exhibit heightened air pollution levels, primarily attributed to temperature inversions. Inversion occurrences involve a layer of warm air confining colder air and pollutants close to the ground, impeding their dispersion into the atmosphere. Unlike summer air pollution, winter conditions result in the prolonged presence of pollutants, increasing the likelihood of higher inhalation rates. This extended exposure raises health concerns for individuals, as reduced ventilation and dispersion contribute to potential health effects.

Air quality near the ground during winter is expected to be dominated by local residential heating emissions with the contribution of vehicle engine exhausts. For this season, the in-situ measurements represent the most viable way to investigate the aerosol distribution and composition, while the deployment of remote sensing instruments (e.g., lidar) is limited by instrumental and environmental factors. During wintertime, the condensation of water droplets (especially during nighttime) along with the recurrent formation of cloud layers attenuate the laser beam, thus impeding the lidar/ceilometer measurements; moreover, even under clear sky conditions, the particulate is usually confined within the first 300 m from the ground (i.e., the typical PBL layer thickness in wintertime), where the active remote sensing techniques are not able to provide reliable results. On the other hand, the in-situ instrumentations enable the analysis of the particulate matter collected at the ground level where the pollutants highly concentrate as a result of the stagnant, dense and cold air. Among the in-situ measurements, aethalometer plays a key role: the BC content of particulate matter originates mostly from the incomplete combustion of both fossil fuel and biomass used as combustibles for domestic heating. The BC content is expected to be higher with respect to the background summer levels, especially due to the contribution of local residential heating and the air stagnation. The BC source apportionment is expected to be determined by both biomass burning fraction due to the residential wood burning and the fossil fuel due to the traffic exhaust and residential heating.

The OC/EC analysis on the $PM_{2.5}$ fraction is expected to provide additional data to both support and integrate the results obtained with the aethalometer (Schmidl et al., 2008; Gonçalves et al., 2010; Pio et al., 2011; Sirignano et al., 2019). The nephelometer is expected to provide the optical parameters at the ground complementing the ones obtained by lidar measurements in the 300 m-UTLS region; the total scattering coefficient σ_{sp} and the backscattering coefficient σ_{bsp} are related to the concentration of particles, with a dominant response expected at 450 nm and relatively high values for the SAE, corresponding to the fine and ultra-fine particles typically produced by heating emissions (Esteve et al., 2012). Further elucidations on the nature and the origin of the particulate can be certainly obtained with the ToF-ACSM. In this case, an accurate prediction of the chemical composition of the particulate is not a trivial task since many factors contribute to the chemistry of the particulate and, as of today, there are no previous data reports for such type of analysis at the site in wintertime. In principle, however, the chemical speciation of the PM_1 fraction from the ACSM is expected to put in evidence a prevalence of the organic matter derived from the combustion processes. Moreover, as previously reported (Chen et al., 2012), during wintertime the recurrent exceedances of the fine particle fractions may be due to the abundance of the secondary ammonium nitrate (NH_4NO_3), attributed to residential wood combustion and diesel engines through the emission of nitrogen oxides (NOx)

https://doi.org/10.5194/amt-2024-57
Preprint. Discussion started: 13 May 2024

Atmospheric Measurement Techniques Discussions

from these sources. Finally, the importance of the chemical analysis of the filters must be underlined; through ICP-OES the main metals present in the particulate can be analyzed (Na, Mg, Al, Ca, V, Cr, Fe, Mn, Ni, Cu, Zn, As, Mo, Sb, Cd, Ba, Pb) which come from specific sources, such as the combustion of fossil fuels in industries or power plants or in vehicle combustion engines, coal and wood combustion processes, non-combustion related emissions from vehicular traffic and dust resuspension phenomena resulting from traffic (Dušan et al., 2017; Zhi et al., 2021).

In the following we investigate the average daily concentration of equivalent black carbon (eBC) obtained by the aethalometer (Figure 8a), covering the period from June 2023 to April 2024, to have a first insights into air quality near the ground during winter. Our analysis reveals no significant increase in eBC concentration during the winter months compared to background levels observed in summer. However, when examining the daily average percentage of black carbon (BC) originating from biomass burning (BB%), as determined by the Sandradewi model, in conjunction with the daily average temperature data obtained from the Vaisala AWS310 weather station situated at the site (Figure 8b), an intriguing trend emerges. It becomes evident that BB% is substantially higher during winter months than during summer months. Given the minimal occurrence of wildfires and prescribed burns at the site during winter, the primary source of biomass burning influence can be attributed to residential burning, a consequence of the notably low temperatures experienced during that period. These first data indicate that the main source of BC during winter at our site is predominantly from local residential heating emissions.

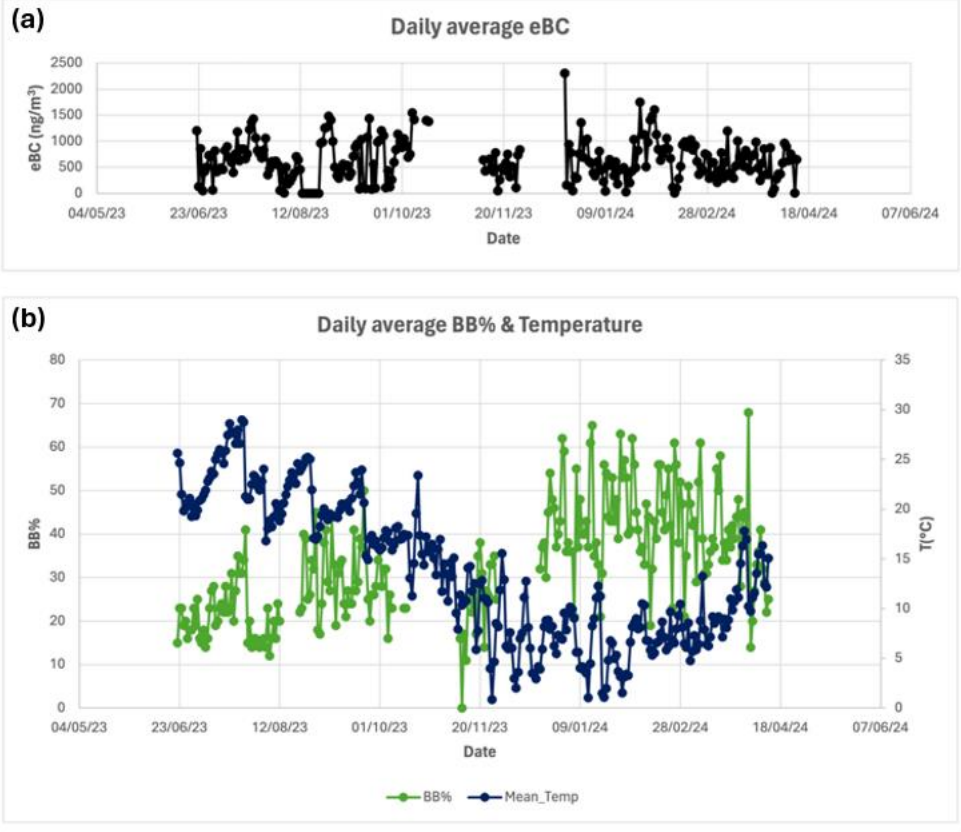

https://doi.org/10.5194/amt-2024-57
Preprint. Discussion started: 13 May 2024

Figure 8: Daily average eBC concentration obtained by aethalometer from June 2023 to April 2024 a), top panel daily average BB% determined by the Sandradewi model from June 2023 to April 2024; bottom panel daily average temperature data obtained from the Vaisala AWS310 weather station from June 2023 to April 2024 b).

5.3 Dust intrusions

During summer and spring, the site is regularly affected by Saharan dust intrusions (Mona et al., 2006). Desert dust particles have many effects: they can impact climate, the precipitation cycle, and human health (Sokolik et al., 2007; Mona et al., 2023). Mineral dust particles can act as cloud condensation nuclei (CCN) and thereby determine the concentration of the initial droplets, albedo, precipitation formation, and lifetime of clouds (Levin et al., 1996; Levin et al., 2005).

The multiwavelength polarisation Raman lidar provides highly resolved spatial and temporal atmospheric profiles that allow for the separation of the different aerosol layers (Pappalardo et al., 2004b; Papagiannopoulos et al., 2018). Large and irregular shaped Saharan desert dust particles produce medium lidar ratios S, relatively high PLDR values and they are spectrally neutral to backscatter and extinction producing low Ångström exponent referred to the wavelengths 355-532 nm (Freudenthaler et al., 2006; Fernandez et al., 2019). In fact, mineral desert dust aerosols predominantly consist of coarse mode particles of irregular shapes (Mahowald et al., 2014).

In-situ measurements, in case of sedimentation events, provide complementary information on the advected dust. Low values of nephelometer-derived SAE that indicate carse particles and, conversely, high aethalometer-derived AAE values that demonstrate the wavelength dependent absorption (Cazorla et al., 2013).

When the atmosphere is dominated by particles with large dimension such as dust particle, the sedimentation is fostered and involves higher return to the ground level so the measurements of size distribution of coarse particles by APS plays a key role in dust studies Furthermore, the low $PM_{2.5}/PM_{10}$ ratio obtained by real time measurements using the PMx monitor could be the confirmation that the main component of the desert dust events is the PM coarse fraction. Finally, the PM_{10} mass concentration collected over 24h on filter measured by the PMx sampler (SWAM 5a-Dual Channel Monitors, FAI Instruments) will be higher during a dust event compared to non-dust events, with PM_{10} concentration values that could exceed the European daily limit value (2008/50/CE European directive).

Regarding the chemical characterization, the ICP-OES plays a key role in evaluating the influence of the transport of dust by detecting the elemental composition of the mineral fraction. In particular, monitoring the concentrations of the typical crustal elements such as As, Al, Ca Cr, Cd, Co, Cu, Fe, K, Mn, Mo, Na, Ni, Pb, Sb, Se, Sn, and Zn and Rare Earth Elements (REEs) is relevant because are generally markedly higher during desert dust event than in comparison with their annual means (Aydin et al., 2012; Rodriguez-Navarro et al.,2018; Mărmureanu et al., 2019).

In the following we report an example of aerosol remote sensing and in-situ observation for a Saharan dust intrusion at CIAO to demonstrate the possibilities for synergistic combination of data from lidar and in-situ aerosol measurements. Even if only the APS instrument was available at that time, the presence of just one in-situ instrumentation already shown the importance

https://doi.org/10.5194/amt-2024-57
Preprint. Discussion started: 13 May 2024


Atmospheric Measurement Techniques Discussions

of such combination of techniques. The observations are related to the second half of June. Figure 9a reports the fine mode fraction as retrieved from CIAO photometer measurements and available at aeronet.gsfc.nasa.gov. This parameter provides information about the fraction of fine mode particles respect to the coarse one as obtained from the AOD (Aerosol optical Depth) measurements. This parameter is retrieved from columnar measurements and therefore refer to the total atmospheric column. Fig 9a clearly shows that in the 20-23 June period the coarse particles are more abundant respect to previous and following period. For the same period Hybrid Single-Particle Lagrangian Integrated Trajectory (HYSPLIT) backward trajectories ending over Potenza indicate Sahara desert as potential source of the observed particles.

Lidar obseravtions provide a better insight of the temporal and vertical distribution of the aerosol at CIAO on those days. Figure 9b-c report available Lidar observations for the period. It shows the color-maps of the vertical distribution and temporal dynamics of the aerosol as time series of range-corrected lidar signals at 532 nm for the night of 22 June 2023 and the daytime day of 23 June 2023. In particular, these plots report the component of backscattered signals at 532 cross-polarized respect to the emitted laser light: the presence of high cross-polarized backscatter signals is a signature of presence in that portion of 4d atmospheric region of aspherical particles, like Saharan dust ones.

The representation of the aerosol distribution during the night of 22 June (Fig. 9b) shows two main layers of dust: one at an altitude close to 1 km above ground level (agl) and a second denser one above it at a height of approximately 3 km agl. Particularly interesting for the potential link with in-situ measurements is a branch of the lower layer around 01:30 in the night between 22 and 23 June, which seems to descent in altitude and could potentially sediment at the ground. It is worth to note that the lidar blind region for the instrument available at the time of the measurements was around 400 m not allowing to further investigate this point. Over the next day (Fig. 9c), the color-map again indicates the presence of dust from 9:00 to 12:00 at similar heights to 22 June but with lower density until it disappears after 12:00.

https://doi.org/10.5194/amt-2024-57
Preprint. Discussion started: 13 May 2024

Atmospheric Measurement Techniques Discussions

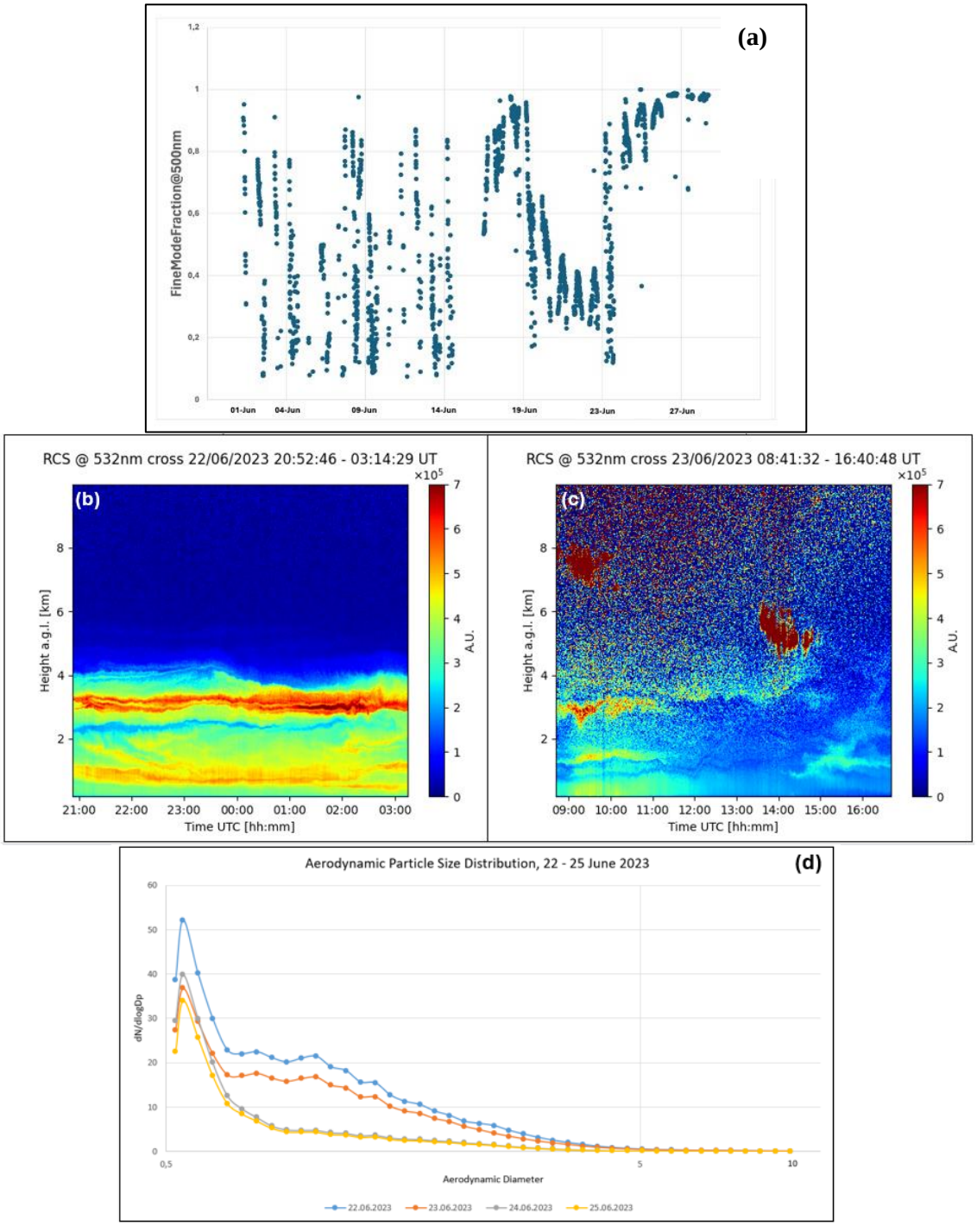

Figure 9: Fine mode fraction as retrieved from CIAO photometer measurements related to the second half of June (a), color-coded time series of range-corrected lidar signals measured at 532 nm cross-polarized channel obtained with the MUSA lidar system on 22 June 2023 (b) and 23 June 2023 (c), aerodynamic particle size distribution daily averages obtained with APS on 22-25 June 2023 (d).

https://doi.org/10.5194/amt-2024-57
Preprint. Discussion started: 13 May 2024


Atmospheric Measurement Techniques Discussions

Online observations at the ground allow a better understanding of the dust presence at the surface exploring also the status after the 22-23 June. In that period, only APS and aethalometer were operational at CIAO.

Fig. 7d shows the aerodynamic particle size distribution daily averages obtained with APS on 22-25 June 2023 and provides complementary information to that obtained through lidar and photometer measurements. Indeed, Fig 7d distinctly illustrates that there is negligible variance in the concentration of ultrafine particulates between dust (22-23 June) and non-dust (24-25 June) days, instead there is a noticeable rise in the concentration of fine and coarse particles with a diameter of up to 5 µm on the dust days (22-23 June) compared to the non-dust days (24- 25 June); demonstrating how during dust events the atmosphere is dominated by large particles (Fig 7a) distributed over different altitude ranges (Fig 7b-c) and if sedimentation is favoured, this leads to a greater return to ground level in the coarse mode (Fig. 7d).

More information would be needed for a deeper investigation of such kind of event, and this is the reason why the CIAO observatory has been extensively upgraded as described in this paper and we surely will observe in the next future other events to be analysed through online and offline instruments. However, this kind of detailed investigation is out of the scope of the current paper and would be object of further publications.

6 Conclusions

The recent upgrade of CIAO with the aerosol in-situ laboratory aims to provide comprehensive data on aerosol composition and properties, which will contribute to improve climate change models and understand the effects on human health and ecosystems. The aerosol in-situ laboratory has started in November 2023 the ACTRIS labelling process in order to prove the operational capacities of the National Facility in ACTRIS and ensure the high quality of ACTRIS data in order to obtain the label “ACTRIS National Facility” for the aerosol in-situ component.

The continuous in-situ measurements in tandem with the aerosol remote sensing suite will provide a valuable record of aerosol observations for synergises. Additionally, an ICOS Atmospheric site is under implementation: this will furthermore enhance CIAO’s observing capabilities and synergies. All data collected are open and available to external users through international databases (e.g., ACTRIS and ICOS) or through CIAO local services (e.g., meteo data). CIAO also offers remote and physical access to the facility (https://ciao.imaa.cnr.it/access-2/), hosting researchers, students, SMEs and stakeholders, but even the possibility to host user’s instruments or sending CIAO mobile platforms to users’ sites. All the above are implemented with the main objective of fostering the advancement of the knowledge in the atmospheric field, through the wide use from the scientific community of such extended CIAO observational datasets.

The CIAO aerosol in-situ laboratory has been built following ACTRIS suggestions and requirements, for which technical solutions and schemas are here reported. The instrumental set up will allow to address main research topics such as the aerosol typing and the characterization of the PBL. A first step towards integrating CIAO’s different observing platforms is planned during an extensive CIAO measurement campaign focused on the estimation of the PBL using aerosol lidar methodologies and its validation with independent measurements and techniques that will be held in Spring 2024. Furthermore, the next-to-

https://doi.org/10.5194/amt-2024-57
Preprint. Discussion started: 13 May 2024


Atmospheric Measurement Techniques Discussions

come ICOS Atmospheric Class 1 site at CIAO (first step of labelled process already passed) will offer other possibilities of synergistic studies and integration among Ris in the environmental filed. In this direction, CIAO is deeply involved in the developments of ITINERIS (Italian Integrated Environmental Research Infrastructures System), an overarching National project for enhancing the interlinkages of all the Italian Ris in the environmental domain. The multi-platform and multi-disciplinary approach of the observatory coupled with the open data and open access philosophy is key for better addressing complex atmospheric and environmental questions posed by climate change and anthropization processes.

Author contributions

TL, AM and ST contributed to Writing – original draft preparation. TL, AM, ST, CCol and MM contributed to Visualization. TL, AM, ST, FC, DA contributed to Methodology. TL and MM contributed to Formal analysis. DA, AG, CD, ER and CC contributed to Resources. CCor, SG, RMAP, GP contributed to Funding acquisition. EL contributed to Software. TL, AM, ST, AA, BDR, MR, LM contributed to Writing - review & editing. FC, EL, FM, DA, AG, CCor, BDR, CD, SG, MM, NP, GP, RMPA, ER, DS and CCol contributed to Review & editing. GP and LM contributed to Conceptualization. LM contributed to Project administration and Supervision.

Competing interests

The authors declare that they have no conflict of interest.

Acknowledgements

The authors acknowledge the MIUR (Italian Ministry of University) PON Ricerca e Innovazione 2014-2020 – PER-ACTRIS-IT – “Potenziamento della componente italiana dell'Infrastruttura di Ricerca Aerosol, Clouds and Trace Gases Research; CIR01_00015 - PER-ACTRIS-IT “Potenziamento della componente italiana della Infrastruttura di Ricerca Aerosol, Clouds and Trace Gases Research Infrastructure - Rafforzamento del capitale umano” - Avviso MUR D.D. n. 2595 del 24.12.2019 Piano Stralcio “Ricerca e Innovazione 2015-2017” and CIR01_00019 - PRO-ICOS_MED “Potenziamento della Rete di Osservazione ICOS-Italia nel Mediterraneo - Rafforzamento del capitale umano” - Avviso MUR D.D. n. 2595 del 24.12.2019 Piano Stralcio “Ricerca e Innovazione 2015-2017”.The authors also acknowledge the IR0000032 – ITINERIS, Italian Integrated Environmental Research Infrastructures System (D.D. n. 130/2022 - CUP B53C22002150006) Funded by EU - Next Generation EU PNRR- Mission 4 “Education and Research” - Component 2: “From research to business” - Investment 3.1: “Fund for the realisation of an integrated system of research and innovation infrastructures” and ATMO-ACCESS (Access to Atmospheric Research Facilities) Funded in the frame of the programme H2020-EU.1.4.1.2 – Grant

673 Agreement n. 101008004 – (1 April 2021 – 31 March 2025)..The authors also acknowledge the Joint Research Unit ACTRIS-
674 Italy funded by the Italian Ministry of University and Research.
675
676 **References**
677
678 Allen, A. G., Nemitz, E., Shi J. P., Harrison R. M., and Greenwood, J. C.: Size distribution of trace metals in atmospheric
679 aerosols in the United Kingdom, Atmos. Environ., 35, 4581–4591, http://dx.doi.org/10.1016/S1352-2310(01)00190-X, 2001.
680 Aydin, F., Aydin, I., Erdoğan, S., Akba, O., Isik, B., & Hamamci, C.: Chemical Characteristics of Settled Particles during a
681 Dust-Storm. Pol. J. Environ. Stud., 21, 533-537, 2012.
682 Atabakhsh, S., Poulain, L., Chen, G., Canonaco, F., Prévôt, A. S. H., Pöhlker, M., Wiedensohler, A., and Herrmann, H.: A 1-
683 year aerosol chemical speciation monitor (ACSM) source analysis of organic aerosol particle contributions from anthropogenic
684 sources after long-range transport at the TROPOS research station Melpitz, Atmos. Chem. Phys., , 23, 6963–6988,
685 https://doi.org/10.5194/acp-23-6963-2023, 2023.
686 Baars, H., Ansmann, A., Ohneiser, K., Haarig, M., Engelmann, R., Althausen, D., Hanssen, I., Gausa, M., Pietruczuk, A.,
687 Szkop, A., Stachlewska, I. S., Wang, D., Reichardt, J., Skupin, A., Mattis, I., Trickl, T., Vogelmann, H., Navas-Guzmán, F.,
688 Haefele, A., Acheson, K., Ruth, A. A., Tatarov, B., Müller, D., Hu, Q., Podvin, T., Goloub, P., Veselovskii, I., Pietras, C.,
689 Haeffelin, M., Fréville, P., Sicard, M., Comerón, A., Fernández García, A. J., Molero Menéndez, F., Córdoba-Jabonero, C.,
690 Guerrero-Rascado, J. L., Alados-Arboledas, L., Bortoli, D., Costa, M. J., Dionisi, D., Liberti, G. L., Wang, X., Sannino, A.,
691 Papagiannopoulos, N., Boselli, A., Mona, L., D'Amico, G., Romano, S., Perrone, M. R., Belegante, L., Nicolae, D., Grigorov,
692 I., Gialitaki, A., Amiridis, V., Soupiona, O., Papayannis, A., Mamouri, R.-E., Nisantzi, A., Heese, B., Hofer, J., Schechner, Y.
693 Y., Wandinger, U., and Pappalardo, G.: The unprecedented 2017–2018 stratospheric smoke event: decay phase and aerosol
694 properties observed with the EARLINET, Atmos. Chem. Phys., 19, 15183–15198, https://doi.org/10.5194/acp-19-15183-
695 2019, 2019.
696 Baltensperger, U., Weingarter, E., Burtscher, H., and Keskinen, J.: Dynamic mass and surface area measurements, in: Aerosol
697 Measurement, edited by: Baron, P.-A., and Willeke, K., Jhon Wiley and Sons, New York, 387-418, 2001.
698 Binietoglou, I., Basart, S., Alados-Arboledas, L., Amiridis, V., Argyrouli, A., Baars, H., Baldasano, J. M., Balis, D., Belegante,
699 L., Bravo-Aranda, J. A., Burlizzi, P., Carrasco, V., Chaikovsky, A., Comerón, A., D'Amico, G., Filioglou, M., Granados-
700 Muñoz, M. J., Guerrero-Rascado, J. L., Ilic, L., Kokkalis, P., Maurizi, A., Mona, L., Monti, F., Muñoz-Porcar, C., Nicolae, D.,
701 Papayannis, A., Pappalardo, G., Pejanovic, G., Pereira, S. N., Perrone, M. R., Pietruczuk, A., Posyniak, M., Rocadenbosch,
702 F., Rodríguez-Gómez, A., Sicard, M., Siomos, N., Szkop, A., Terradellas, E., Tsekeri, A., Vukovic, A., Wandinger, U., and
703 Wagner, J.: A methodology for investigating dust model performance using synergistic EARLINET/AERONET dust
704 concentration retrievals, Atmos. Meas. Tech., 8, 3577–3600, https://doi.org/10.5194/amt-8-3577-2015, 2015.

705 Boselli, A., Caggiano, R., Cornacchia, C., Madonna, F., Macchiato, M., Mona, L., Pappalardo, G., and Trippetta, S.: Multi
706 year sun-photometer measurements for aerosol characterization in a Central Mediterranean site, Atmos. Res., 104, 98–110,
707 https://doi:10.1016/j.atmosres.2011.08.002, 2012.
708 Bressi, M., Cavalli, F., Putaud, J. P., Fröhlich, R., Petit, J. E., Aas, W., Äijälä, M., Alastuey, A., Allan, J. D., Aurela, M., Beric,
709 M., Bougiatioti, A., Bukowiecki, N., Canonaco, F., Crenn, V., Dusanter, S., Ehn, M., Elsasser, M. and Prevot, A. S. H.: A
710 European aerosol phenomenology - 7: High-time resolution chemical characteristics of submicron particulate matter across
711 Europe, Atmos. Environ., 10, 100108 https://doi.org/10.1016/j.aeaoa.2021.100108, 2021.
712 Cavalli, F., Viana, M., Yttri, K. E., Genberg, J., and Putaud, J. P.: Toward a standardised thermal-optical protocol for measuring
713 atmospheric organic and elemental carbon: the EUSAAR protocol, Atmos. Meas. Tech., 3, 79–89, https://doi.org/10.5194/amt-
714 3-79-2010, 2010.
715 Cazorla, A., Bahadur, R., Suski, K. J., Cahill, J. F., Chand, D., Schmid, B., Ramanathan, V., and Prather, K. A.: Relating
716 aerosol absorption due to soot, organic carbon, and dust to emission sources determined from in-situ chemical measurements,
717 Atmos. Chem. Phys., 13, 9337–9350, https://doi.org/10.5194/acp-13-9337-2013, 2013.
718 Chen, L. W. A., Watson, J. G., Chow, J. C., Green, M. C., Inouye, D., and Dick, K.: Wintertime particulate pollution episodes
719 in an urban valley of the Western US: a case study, Atmos. Chem. Phys., 12, 10051–10064, https://doi.org/10.5194/acp-12-
720 10051-2012, 2012.
721 Cubison, M. J., Ortega, A. M., Hayes, P. L., Farmer, D. K., Day, D., Lechner, M. J., Brune, W. H., Apel, E., Diskin, G. S.,
722 Fisher, J. A., Fuelberg, H. E., Hecobian, A., Knapp, D. J., Mikoviny, T., Riemer, D., Sachse, G. W., Sessions, W., Weber, R.
723 J., Weinheimer, A. J., Wisthaler, A., and Jimenez, J. L.: Effects of aging on organic aerosol from open biomass burning smoke
724 in aircraft and laboratory studies, Atmos. Chem. Phys., 11, 12049–12064, https://doi.org/10.5194/acp-11-12049-2011, 2011.
725 De Rosa, B., Amato, F., Amodeo, A., D'Amico, G., Dema, C., Falconieri, A., Giunta, A., Gumà-Claramunt, P., Kampouri, A.,
726 Solomos, S., Mytilinaios, M., Papagiannopoulos, N., Summa, D., Veselovskii, I.; Mona, L.: Characterization of Extremely
727 Fresh Biomass Burning Aerosol by Means of Lidar Observations, Remote Sens., 14, 4984, https://doi.org/10.3390/rs14194984,
728 2022.
729 Drinovec, L., Močnik, G., Zotter, P., Prévôt, A.-S.-H., Ruckstuhl, C., Coz, E., Rupakheti, M., Sciare, J., Müller, T.,
730 Wiedensohler, A., and Hansen, A. D.: The "dual-spot" Aethalometer: an improved measurement of aerosol black carbon with
731 real-time loading compensation, Atmos. Meas. Tech., 8, 1965–1979, https://doi.org/10.5194/amt-8-1965-2015, 2015.
732 Dušan, J., Ďurčanská, D., Bujdos. M.: The contribution of road traffic to particulate matter and metals in air pollution in the
733 vicinity of an urban road, Transport and Environment, 50, 397-408, https://doi: 10.1016/j.trd.2016.11.024, 2017
734 Esteve, A. R., Estellés, V., Utrillas, M. P., Martínez-Lozano, J. A.: In-situ integrating nephelometer measurements of the
735 scattering properties of atmospheric aerosols at an urban coastal site in western Mediterranean, Atmos. Environ., 47, 43–50,
736 https://doi.org/10.1016/j.atmosenv.2011.11.043, 2012.
737 Fernandez, A. J., Sicard, M., Costa, M. J., Guerrero-Rascado, J. L., Gómez-Amo, J. L., Molero, F., Barragán, R., Basart, S.,
738 Bortoli, D., Bedoya-Velásquez, A. E., Utrillas, M. P., Salvador, P., Granados-Muñoz, M. J., Potes, M., Ortiz-Amezcua, P.,

739 Martínez-Lozano, J. A., Artíñano, B., Muñoz-Porcar, C., Salgado, R., Román, R., Rocadenbosch, F., Salgueiro, V., Benavent-
740 Oltra, J. A., Rodríguez-Gómez, A., Alados-Arboledas, L., Comerón, A., and Pujadas, M.: Extreme, wintertime Saharan dust
741 intrusion in the Iberian Peninsula: lidar monitoring and evaluation of dust forecast models during the February 2017 event,
742 Atmos. Res., 228, 223–241, https://doi.org/ 10.1016/j.atmosres.2019.06.007, 2019.
743 Freudenthaler, V., Esselborn, M., Wiegner, M., Heese, B., Tesche, M., Ansmann, A., Müller, D., Althausen, D., Wirth, M.,
744 Fix, A., Ehret, G., Knippertz, P., Toledano, C., Gasteiger, J., Garhammer, M., and Seefeldner, M.: Depolarization ratio profiling
745 at several wavelengths in pure Saharan dust during SAMUM 2006, Tellus B., 61, 165–179, https://doi.org/10.1111/j.1600-
746 0889.2008.00396.x, 2009.
747 Fröhlich, R., Cubison, M. J., Slowik, J. G., Bukowiecki, N., Prévôt, A. S. H., Baltensperger, U., Schneider, J., Kimmel, J. R.,
748 Gonin, M., Rohner, U., Worsnop, D. R., and Jayne, J. T.: The ToF-ACSM: a portable aerosol chemical speciation monitor
749 with TOFMS detection, Atmos. Meas. Tech., 6 (11), 3225–3241, https://doi.org/10.5194/amt-6-3225-2013, 2013.
750 Gonçalves, C., Alves, C., Evtyugina, M., Mirante, F., Pio, C., Caseiro, A., Schmidl, C., Bauer, H., Carvalho, F.:
751 Characterisation of PM10 emissions from wood-stove combustion of common woods grown in Portugal, Atmos. Environ., 44,
752 4474-4480, https://doi.org/10.1016/j.atmosenv.2010.07.026, 2010.
753 http://rsdi.regione.basilicata.it, last access: 28 November 2023.
754 https://www.actris.eu, last access: 13 December 2023.
755 https://www.atmo-access.eu/second-call-for-access/, last access: 2 December 2023.
756 https://ciao.imaa.cnr.it, last access: 4 December 2023.
757 https://www.imaa.cnr.it/en/projects/38-attivita/progetti/713-per-actris-it, last access: 6 December 2023.
758 https://www.permapure.com, last access: 10 December 2023.
759 Huang, R. J., Yang, L., Cao, J., Chen, Y., Chen, Q., Li, Y., Duan, J., Zhu, C., Dai, W., Wang, K.: Browncarbonaerosol
760 inurbanXi'an, northwest china: The composition and light absorption properties. Environ. Sci. Technol, 52(12), 6825–33.
761 https://doi:10.1021/acs.est.8b02386, 2018.
762 Ilić, L., Jovanović, A., Kuzmanoski, M., Lazić, L., Madonna, F., Rosoldi, M., Mytilinaios, M., Marinou, E., and Ničković, S.:
763 Mineralogy sensitive immersion freezing parameterization in DREAM, J. Geophys. Res. Atmos., 127, e2021JD035093,
764 https://doi.org/10.1029/2021JD035093, 2022.
765 Kim, H. K., Choi, Y., and Ghim, Y. S.: Characterization of volatilization of filter-sampled PM2.5 semi-volatile inorganic ions
766 using a backup filter and denuders, Aerosol Air Qual. Res., 15, 814–820, https://doi.org/10.4209/aaqr.2014.09.0213, 2015.
767 Levin, Z., Ganor, E., and Gladstein, V.: The effects of desert particles coated with sulphate on rain formation in the Eastern
768 Mediterranean, J. Appl. Meteorol., 35, 1511–1523, https://doi.org/10.1175/15200450(1996)035<1511:TEODPC>2.0.CO;2,
769 1996.
770 Levin, Z., Teller, A., Ganor, E. and Yin, Y.: On the interactions of mineral dust, sea-salt particles, and clouds: a measurement
771 and modeling study from the Mediterranean Israeli Dust Experiment campaign, J. Geophys. Res., 110, D20202,
772 https://doi.org/10.1029/2005JD005810, 2005.

773 Lopatin, A., Dubovik, O., Chaikovsky, A., Goloub, P., Lapyonok, T., Tanré, D., and Litvinov, P.: Enhancement of aerosol
774 characterization using synergy of lidar and sun-photometer coincident observations: the GARRLiC algorithm, Atmos. Meas.
775 Tech., 6, 2065–2088, https://doi.org/10.5194/amt-6-2065-2013, 2013.
776 Madonna, F., Amodeo, A., Cornacchia, C., D'Amico, G., Mona, L., Pandolfi, M., Pappalardo, G., and Cuomo, V.:
777 Multichannel microwave radiometer and water vapour Raman lidar: comparisons and synergies, AITinforma - Rivista Italiana
778 di telerilevamento, 35, 115–130, 2006.
779 Madonna F., Amodeo, A., D'Amico, G., Mona, L., and Pappalardo, G.: Observation of non-spherical ultragiant aerosol using
780 a microwave radar, Geophys. Res. Lett., 37, L21814, doi:10.1029/2010GL044999, 2010.
781 Madonna, F., Amodeo, A., Boselli, A., Cornacchia, C., Cuomo, V., D'Amico, G., Giunta, A., Mona, L., and Pappalardo, G.:
782 CIAO: the CNR-IMAA advanced observatory for atmospheric research, Atmos. Meas. Tech., 4, 1191–1208,
783 https://doi.org/10.5194/amt-4-1191-2011, 2011.
784 Madonna, F., Amodeo, A., D'Amico, G., and Pappalardo, G.: A study on the use of radar and lidar for characterizing ultragiant
785 aerosol, J. Geophys. Res. Atmos., 118, doi:10.1002/jgrd.50789, 2013.
786 Madonna, F., Amato, F., Vande Hey, J., and Pappalardo, G.: Ceilometer aerosol profiling versus Raman lidar in the frame of
787 the INTERACT campaign of ACTRIS, Atmos. Meas. Tech., 8, 2207–2223, https://doi.org/10.5194/amt-8-2207-2015, 2015.
788 Mahowald, N., Albani, S., Kok, J. F., Engelstaeder, S., Scanza, R., Ward, D. S. and Flanner, M. G.: The size distribution of
789 desert dust aerosols and its impact on the Earth system, Aeolian Res., 15, 53–71, https://doi.org/10.1016/j.aeolia.2013.09.002,
790 2014.
791 Mamouri, R.-E., and Ansmann, A.: Potential of polarization lidar to provide profiles of CCN- and INP-relevant aerosol
792 parameters, Atmos. Chem. Phys., 16, 5905–5931, https://doi.org/10.5194/acp-16-5905-2016, 2016.
793 Mamouri, R.-E., and Ansmann, A.: Potential of polarization/Raman lidar to separate fine dust, coarse dust, maritime, and
794 anthropogenic aerosol profiles, Atmos. Meas. Tech., 10, 3403–3427, https://doi.org/10.5194/amt-10-3403-2017, 2017.
795 Mărmureanu, L., Marin, C.A., Andrei, S., Antonescu, B., Ene, D., Boldeanu, M., Vasilescu, J., Viţelaru, C., Cadar, O., Levei,
796 E.: Orange Snow—A Saharan Dust Intrusion over Romania During Winter Conditions. Remote Sens., 11, 2466.
797 https://doi.org/10.3390/rs11212466, 2019
798 Matthias, V., Balis, D., Bosenberg, J., Eixmann, R., Iarlori, M., Komguem, L., Mattis, I., Papayannis, A., Pappalardo, G.,
799 Perrone, M. R., and Wang, X.: Vertical aerosol distribution over Europe: Statistical analysis of Raman lidar data from 10
800 European Aerosol Research Lidar Network (EARLINET) stations, J. Geophys. Res. Atmos., 109 (D18), D18201,
801 https://doi.org/10.1029/2004JD004638, 2004.
802 Middlebrook, A. M., Bahreini, R., Jimenez, J. L., and Canagaratna, M. R.: Evaluation of composition-dependent collection
803 efficiencies for the Aerodyne Aerosol Mass Spectrometer using field data, Aerosol Sci. Tech., 46, 258–271,
804 https://doi.org/10.1080/02786826.2011.620041, 2012.

Molero, F., Pujadas, M., and Artinano, B.: Study of the Effect of Aerosol Vertical Profile on Microphysical Properties Using GRASP Code with Sun/Sky Photometer and Multiwavelength Lidar Measurements, Remote Sens., 12(24) 4072-4089, https://doi.org/10.3390/rs12244072, 2020.

Mona, L., Amodeo, A., Pandolfi, M., and Pappalardo, G.: Saharan dust intrusions in the Mediterranean area: three years of Raman lidar measurements, J. Geophys. Res., 111, D16203, https://doi:10.1029/2005JD006569, 2006.

Mona, L., Pappalardo, G., Amodeo, A., D'Amico, G., Madonna, F., Boselli, A., Giunta, A., Russo, F., and Cuomo, V.: One year of CNR-IMAA multi-wavelength Raman lidar measurements in coincidence with CALIPSO overpasses: Level 1 products comparison, Atmos. Chem. Phys., 9, 7213–7228, https://doi:10.5194/acp-9-7213-2009, 2009.

Mona, L., Amodeo, A., D'Amico, G., Giunta, A., Madonna, F., and Pappalardo, G.: Multi-wavelength Raman lidar observations of the Eyjafjallajökull volcanic cloud over Potenza, southern Italy, Atmos. Chem. Phys., 12, 2229-2244, https://doi:10.5194/acp-12-2229-2012, 2012.

Mona, L., Papagiannopoulos, N., Basart, S., Baldasano, J., Binietoglou, I., Cornacchia, C., and Pappalardo, G.: EARLINET dust observations vs. BSC-DREAM8b modeled profiles: 12-year-long systematic comparison at Potenza, Italy, Atmos. Chem. Phys., 14, 8781–8793, https://doi.org/10.5194/acp-14-8781-2014, 2014.

Mona, L., Amiridis, V., Cuevas, E., Gkikas, A., Trippetta, S., Vendenbussche, S., Benedetti, a., Dagsson-Waldhauserova, P., Formenti, P., Haefele, A., Kazadzis, S., Knippertz, P., Laurent, B., Madonna, F., Nickovic, S., Papagiannopoulos, N., Pappalardo, G., García-Pando, C. P., Popp, T., Rodríguez, S., Sealy, A., Sugimoto, N., Terradellas, E., Vimic, A. V., Weinzieri, B., Basart, S.: Observing Mineral Dust in Northern Africa, the Middle East, and Europe: Current Capabilities and Challenges ahead for the Development of Dust Services. *Bull. Amer. Meteor. Soc.*, 104, E2223–E2264, https://doi.org/10.1175/BAMS-D-23-0005.1, 2023.

Monteiro, A., Basart, S., Kazadzis, S., Votsis, A., Gkikas, A., Vandenbussche, S., Tobias, A., Gama, C., García-Pando, C. P., Terradellas, E., Notas, G., Middleton, N., Kushta, J., Amiridis, V., Lagouvardos, K., Kosmopoulos, P., Kotroni, V., Kanakidou, M., Mihalopoulos, N., Kalivitis, N., Dagsson-Waldhauserová, P., El-Askary, H., Sievers, K., Giannaros, T., Mona, L., Hirtl, M., Skomorowski, P., Virtanen, T.H., Christoudias, T., Di Mauro, B., Trippetta, S., Kutuzov, S., Meinander, O., Nickovic, S.: Multi-sectoral impact assessment of an extreme African dust episode in the Eastern Mediterranean in March 2018, Sci Total Environ., 843, 156861. doi: 10.1016/j.scitotenv.2022.156861, 2022.

Nelson, J., Chalbot, M-CG., Tsiodra, I., Mihalopoulos, N., Kavouras, IG.: Physicochemical characterizationofpersonal exposurestosmokeaerosolandPAHsof wildland firefighters inprescribed fires. Expo.Health., 13, 105–18 https://doi:10.1007/s12403-020-00366-5, 2021.

Ng, N. L., Herndon, S. C., Trimborn, A., Canagaratna, M. R., Croteau, P. L., Onasch, T. B., Sueper, D., Worsnop, D. R., Zhang, Q., Sun, Y. L., and Jayne, J. T.: An aerosol chemical speciation monitor (ACSM) for routine monitoring of the composition and mass concentrations of ambient aerosol, Aerosol Sci. Tech., 45 (7), 780–794, https://doi.org/10.1080/02786826.2011.560211, 2011.

838 Nicolae, D., Vasilescu, J., Talianu, C., Binietoglou, I., Nicolae, V., Andrei, S., and Antonescu, B.: A neural network aerosol-
839 typing algorithm based on lidar data, Atmos. Chem. Phys., 18, 14511–14537, https://doi.org/10.5194/acp-18-14511-2018,
840 2018.
841 Ohneiser, K., Ansmann, A., Chudnovsky, A., Engelmann, R., Ritter, C., Veselovskii, I., Baars, H., Gebauer, H., Griesche, H.,
842 Radenz, M., Hofer, J., Althausen, D., Dahlke, S., and Maturilli, M.: The unexpected smoke layer in the High Arctic winter
843 stratosphere during MOSAiC 2019–2020, Atmos. Chem. Phys., 21, 15783–15808, https://doi.org/10.5194/acp-21-15783-
844 2021, 2021.
845 Olson,M.R., VictoriaGarcia, M., Robinson, M. A., Van Rooy, P., Dietenberger, M. A., Bergin, M., Schaue J. J.:.
846 Investigationof blackandbrowncarbonmultiplewavelength-dependent lightabsorptionfrombiomassand fossil fuel
847 combustionsource emissions. J.Geophys. Res. Atmos, 120, 6682–97 https://doi:10.1002/2014JD022970, 2015.
848 Pacifico, L. R., Pizzolante, A., Guarino, A., Iannone, A., Esposito, M., Albanese, S.: Wildfire as a Source of Potentially Toxic
849 Elements (PTSe) in Soil: A Case Study from Campania Region (Italy), Int. J. Environ. Res. Public Health, 20, 4513,
850 https://doi.org/10.3390/ijerph20054513, 2023.
851 Pakkanen, T. A., Loukkola, K., Korhonen, C. H., Aurela, M., Makela, T., Hillamo, R. E., Aarnio, P., Koskentalo, T., Kousa,
852 A. and Maenhaut, W.: Sources and chemical composition of atmospheric fine and coarse particles in the Helsinki area, Atmos.
853 Environ., 35, 5381–5391, http://hdl.handle.net/1854/LU-138499, 2001.
854 Papagiannopoulos, N., Mona, L., Amodeo, A., D'Amico, G., Gumà Claramunt, P., Pappalardo, G., Alados-Arboledas, L.,
855 Guerrero-Rascado, J. L., Amiridis, V., Kokkalis, P., Apituley, A., Baars, H., Schwarz, A., Wandinger, U., Binietoglou, I.,
856 Nicolae, D., Bortoli, D., Comerón, A., Rodríguez-Gómez, A., Sicard, M., Papayannis, A., and Wiegner, M.: An automatic
857 observation-based aerosol typing method for EARLINET, Atmos. Chem. Phys., 18, 15879–15901,
858 https://doi.org/10.5194/acp-18-15879-2018, 2018.
859 Pappalardo, G., Amodeo, A., Mona, L., Pandolfi, M., Pergola, N., and Cuomo, V.: Raman lidar observations of aerosol emitted
860 during the 2002 Etna eruption, Geophys. Res. Lett., 31, L05120, https://doi:10.1029/2003GL019073, 2004a.
861 Pappalardo G., Amodeo, A., Pandolfi, M., Wandinger, U., Ansmann, A., Bosenberg, J., Matthias, V., Amiridis, V., de Tomasi,
862 F., Frioud, M., Iarlori, M., Komguem, L., Papayannis, A., Rocadenbosch, F., and Wang, X.: Aerosol lidar intercomparison in
863 the framework of EARLINET, Part III. Raman lidar algorithm for aerosol extinction, backscatter and lidar ratio, Appl. Opt.,
864 43(28), 5370–5385, https://doi.org/10.1364/AO.43.000977, 2004b.
865 Pappalardo, G., Mona, L., D'Amico, G., Wandinger, U., Adam, M., Amodeo, A., Ansmann, A., Apituley, A., Alados
866 Arboledas, L., Balis, D., Boselli, A., Bravo-Aranda, J. A., Chaikovsky, A., Comeron, A., Cuesta, J., De Tomasi, F.,
867 Freudenthaler, V., Gausa, M., Giannakaki, E., Giehl, H., Giunta, A., Grigorov, I., Groß, S., Haeffelin, M., Hiebsch, A., Iarlori,
868 M., Lange, D., Linné, H., Madonna, F., Mattis, I., Mamouri, R-E., McAuliffe, M. A. P., Mitev, V., Molero, F., Navas-Guzman,
869 F., Nicolae, D., Papayannis, A., Perrone, M. R., Pietras, C., Pietruczuk, A., Pisani, G., Preißler, J., Pujadas, M., Rizi, V., Ruth,
870 A. A., Schmidt, J., Schnell, F., Seifert, P., Serikov, I., Sicard, M., Simeonov, V., Spinelli, N., Stebel, K., Tesche, M., Trickl,

T., Wang, X., Wagner, F., Wiegner, M., Wilson, K. M.: Four-dimensional distribution of the 2010 Eyjafjallajökull volcanic cloud over Europe observed by EARLINET, Atmos. Chem. Phys., 13, 4429-4450, doi:10.5194/acp-13-4429-2013, 2013.

Peters, T. M., and Leith, D.: Concentration measurement and counting efficiency of the aerodynamic particle sizer 3321, J. Aerosol Sci., 34(5), 627-634, https://doi.org/10.1016/S0021-8502(03)00030-2, 2003.

Petzold, A., Ogren, J. A., Fiebig, M., Laj, P., Li, S. M., Baltensperger, U., Holzer-Popp, T., Kinne, S., Pappalardo, G., Sugimoto, N., Wehrli, C., Wiedensohler, A., and Zhang, X. Y.: Recommendations for reporting "black carbon" measurements, Atmos. Chem. Phys., 13, 8365–8379, https://doi.org/10.5194/acp-13-8365-2013, 2013.

Pio, C., Cerqueira, M., Harrison, R. M., Nunes, T., Mirante, F., Alves, C., Oliveira, C., Sanchez de la Campa, A., Artíñano, B., and Matos, M.: OC/EC ratio observations in Europe: Re-thinking the approach for apportionment between primary and secondary organic carbon, Atmos. Environ., 45, 6121–6132, https://doi.org/10.1016/j.atmosenv.2011.08.045, 2011.

Pöschl, U.: Atmospheric Aerosols: Composition, Transformation, Climate and Health Effects. Angew. Chem. Int. Ed., 44: 7520-7540. https://doi.org/10.1002/anie.200501122, 2005.

Rajšić, S., Mijić, Z., Tasić, M., Radenković, M., and Joksić, J.: Evaluation of the levels and sources of trace elements in urban particulate matter, Environ. Chem. Lett., 6, 95–100, https://doi.org/10.1007/s10311-007-0115-0, 2008.

Ridolfi, M., Blum, U., Carli, B., Catoire, V., Ceccherini, S., Claude, H., De Clercq, C., Fricke, K. H., Friedl-Vallon, F., Iarlori, M., Keckhut, P., Kerridge, B., Lambert, J.-C., Meijer, Y. J., Mona, L., Oelhaf, H., Pappalardo, G., Pirre, M., Rizi, V., Robert, C., Swart, D., von Clarmann, T., Waterfall, A., and Wetzel, G.: Geophysical validation of temperature retrieved by the ESA processor from MIPAS/ENVISAT atmospheric limb-emission measurements, Atmos. Chem. Phys., 7, 4459–4487, https://doi.org/10.5194/acp-7-4459-2007, 2007.

Rodriguez-Navarro, C., di Lorenzo, F., and Elert, K.: Mineralogy and physicochemical features of Saharan dust wet deposited in the Iberian Peninsula during an extreme red rain event, Atmos. Chem. Phys., 18, 10089–10122, https://doi.org/10.5194/acp-18-10089-2018, 2018.

Rosoldi, M., Coppa, G., Merlone, A., Musacchio, C., and Madonna, F.: Intercomparison of Vaisala RS92 and RS41 Radiosonde Temperature Sensors under Controlled Laboratory Conditions, Atmosphere, 13, 773, https://doi.org/10.3390/atmos13050773, 2022.

Sandradewi, J., Prévôt, A. S. H., Szidat, S., Perron, N., Alfarra, M., Lanz, V. A., Weingartner, E., and Baltensperger, U.: Using Aerosol Light Absorption Measurements for the Quantitative Determination of Wood Burning and Traffic Emission Contributions to Particulate Matter, Environ. Sci. Technol., 42, 3316–3323, https://doi.org/10.1021/es702253m, 2008.

Sawamura, P., Vernier, J. P., Barnes, J. E., Berkoff, T. A., Welton, E. J., Alados-Arboledas, L., Navas-Guzmán, F., Pappalardo, G., Madonna, F.: Stratospheric AOD after the 2011 eruption of Nabro volcano measured by lidar over the Northern Hemisphere, Environ. Res. Lett., 7, 031001, https://doi.org/ 10.1088/1748-9326/7/3/034013, 2012.

Schmid, O., Karg, E., Hagen, D. E., Whitefield, P. D., and Ferron, G. A.: On the effective density of non-spherical particles as derived from combined measurements of aerodynamic and mobility equivalent size, J. Aerosol Sci., 38(4), 431-443, https://doi.org/10.1016/j.jaerosci.2007.01.002, 2007.

905 Schmidl, C., Marr, I. L., Caseiro, A., Kotianová, P., Berner, A., Bauer, H., Kasper-Giebl, A., Puxbaum, H.: Chemical
906 characterization of fine particle emissions from wood stove combustion of common woods growing in mid-European Alpine
907 regions, Atmos. Environ., 42, 126–141, https://doi.org/10.1016/j.atmosenv.2007.09.028, 2008.
908 Sirignano, C., Riccio, A., Chianese, E., Ni, H., Zenker, K., D'Onofrio, A., Meijer, H. A. J., and Dusek, U.: High Contribution
909 of Biomass Combustion to PM2.5 in the City Centre of Naples (Italy), Atmosphere, 10, 451,
910 https://doi.org/10.3390/atmos10080451, 2019.
911 Sokolik, I. N., and Toon, O. B.: Direct radiative forcing by anthropogenic airborne mineral aerosols, Nature, 381, 681–683,
912 https://doi.org/10.1038/381681a0, 1996.
913 Soupiona, O., Papayannis, A., Kokkalis, P., Foskinis, R., Sánchez Hernández, G., Ortiz-Amezcua, P., Mylonaki, M.,
914 Papanikolaou, C.-A., Papagiannopoulos, N., Samaras, S., Groß, S., Mamouri, R.-E., Alados-Arboledas, L., Amodeo, A., and
915 Psiloglou, B.: EARLINET observations of Saharan dust intrusions over the northern Mediterranean region (2014–2017):
916 properties and impact on radiative forcing, Atmos. Chem. Phys., 20, 15147–15166, https://doi.org/10.5194/acp-20-15147-
917 2020, 2020.
918 Veselovskii, I., Dubovik, O., Kolgotin, A., Korenskiy, M., Whiteman, D. N., Allakhverdiev, K., and Huseyinoglu, F.: Linear
919 estimation of particle bulk parameters from multi-wavelength lidar measurements, Atmos. Meas. Tech., 5, 1135–1145,
920 doi:10.5194/amt-5-1135-2012, 2012.
921 Viana, M., Chi, X., Maenhaut, W., Cafmeyer, J., Querol, X., Alastuey, A., Mikuška, P., and Večeřa, Z.: Influence of sampling
922 artefacts on measured PM, OC, and EC Levels in carbonaceous aerosols in an urban area, Aerosol Sci. Tech., 40 (2), 107–117,
923 https://doi.org/10.1080/02786820500484388, 2006.
924 Villani, M. G., Mona, L., Maurizi, A., Pappalardo, G., Tiesi, A., Pandolfi, M., D'Isidoro, M., Cuomo, V., Tampieri, F.:
925 Transport of volcanic aerosol in the troposphere: the case study of the 2002 Etna plume, J. Geophys. Res., Vol. 111, No. D21,
926 D21102, doi:10.1029/2006JD007126, 2006.
927 Vratolis, S., Fetfatzis, P., Argyrouli, A., Soupiona, O., Mylonaki, M., Maroufidis, J., Kalogridis, A. C., Manousakas, M.,
928 Bezantakos, S., Binietoglou, I., Labzovskii, L. D., Solomos, S., Papayannis, A., Močnik, G., O'Connor, E., Müllerf, D.,
929 Tzanisl, C. G., and Eleftheriadis, K.: Comparison and complementary use of in situ and remote sensing aerosol measurements
930 in the Athens Metropolitan Area, Atmos. Environ., 228 (117439), https://doi.org/10.1016/j.atmosenv.2020.117439, 2020.
931 Wiedensohler, A., Birmili, W., Putaud, J. P., and Ogren, J.: Recommendations for Aerosol Sampling, in: Aerosol Science:
932 Technology and Applications, First Edition, edited by: Colbeck, I., and Lazaridis, M., John Wiley & Sons, Ltd., 45–59,
933 https://doi.org/10.1002/9781118682555.ch3, 2014.
934 Wiegner, M., Madonna, F., Binietoglou, I., Forkel, R., Gasteiger, J., Geiß, A., Pappalardo, G., Schäfer, K., and Thomas, W.:
935 What is the benefit of ceilometers for aerosol remote sensing? An answer from EARLINET, Atmos. Meas. Tech., 7, 1979–
936 1997, https://doi:10.5194/amt-7-1979-2014, 2014.
937 WMO/GAW Aerosol Measurement Procedures, Guidelines and Recommendations 2nd Edition, No. 227, 2016.

https://doi.org/10.5194/amt-2024-57
Preprint. Discussion started: 13 May 2024


Atmospheric Measurement Techniques Discussions

938 Zhi, M., Zhang, X., Zhang, K., Ussher, S. J., Lv, W., Li, J., Gao, J., Luo, Y., Meng, F.,: The characteristics of atmospheric
939 particles and metal elements during winter in Beijing: Size distribution, source analysis, and environmental risk assessment,
940 Ecotoxicol. Environ. Saf., 211, 111937, https://doi.org/10.1016/j.ecoenv.2021.111937, 2021.
941 Zhou, C. W., Huang, H., and Cao, J. J.: Summary of basic characteristics of atmospheric aerosol carbonaceous, Environ. Pollut.
942 Control, 28, 270-274, 2006.
943 Zhao, Q., Huob, J., Yanga, X., Fub, Q., Duanb, Y., Liua, Y., Linb, Y., Zhang, Q.: Chemical characterization and source
944 identification of submicron aerosols from a year-long real-time observation at a rural site of Shanghai using an Aerosol
945 Chemical Speciation Monitor, Atmos. Res., 246, 105154, https://doi.org/10.1016/j.atmosres.2020.105154, 2020.
946